

pubs.acs.org/CR Review

A B B

C

D

E E

G

J

K

Ν

Ν

Ν

0

Ρ

Q

# Optimization of Catalysts and Conditions in Gold(I) Catalysis—Counterion and Additive Effects

Zhichao Lu, Tingting Li, Sagar R. Mudshinge, Bo Xu,\* and Gerald B. Hammond\*



Cite This: https://dx.doi.org/10.1021/acs.chemrev.0c00713

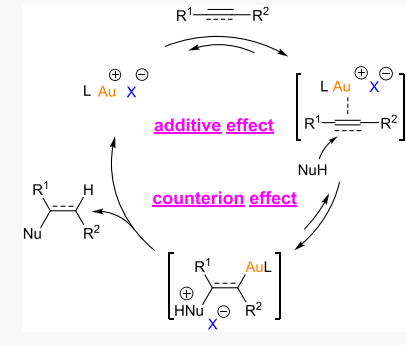


ACCESS

Metrics & More

Article Recommendations

ABSTRACT: Gold catalysis has proven to be an important breakthrough for organic synthesis. The tunable nature of gold catalysts, the unique properties of gold, and the mild reaction conditions required in many gold-catalyzed reactions have all contributed substantially to this metal's popularity in catalysis. However, gold-catalyzed reactions still suffer from limitations such as low turnover numbers (TON). Optimization of the catalysts and reaction conditions may significantly improve the efficiency of gold-catalyzed reactions. In this review, we will present leading examples of counterion or additive-regulated gold catalysis from a mechanistic perspective. We will pay special attention to the physical properties of counterion/additive, such as gold affinity and hydrogen bond basicity, and discuss their effects on the reactivity of gold catalysts.



### **CONTENTS**

. Introduction	
1.1. Fundamentals of Cationic Gold Catalysis	
1.2. Scope and Organization of the Review	
2. Counterion Effect	
2.1. Classification of Counterions	
2.2. Physical Properties of Counterion Affecting	
Reactivities	
2.3. Gold Affinity and Proton-Affinity and Hydro-	
gen Bond Basicity Scale of Counterions	
2.4. Counterion Effects on Reactivity and	
Chemo-/Regioselectivity	
2.4.1. Effect of Counterions on Reactivity	
2.4.2. Effect of Counterions on Chemo-/Regio-	
selectivity	
2.5. Additional Computational Studies on the	
Role of Counterion as Hydrogen Bond	
Acceptors	
2.6. Chiral Counterion Enabled Asymmetric Re-	
actions	

4. Synergistic Effect by Ligand, Counterion, And Additives: A Case Study of Bulk and Green Gold	
Catalysis	Т
5. Conclusion and Outlook	U
Author Information	U
Corresponding Authors	U
Authors	U
Notes	U
Biographies	U
Acknowledgments	U
Abbreviations	U
References	V

### 1. INTRODUCTION

### 1.1. Fundamentals of Cationic Gold Catalysis

Few metals in human history have played such an important role as gold. Besides its ubiquity in jewelry and currency, gold has many indispensable applications in electronics, medicine, dentistry, aerospace, glassmaking, etc. However, homogeneous gold catalysis only provoked enthusiasm among synthetic chemists in the last two decades. 1–7 This enthusiasm is evidenced by an exponential increase in the number of reports

Special Issue: Gold Chemistry

Received: July 7, 2020



3. Additive Effects

Generation

Reactivations

3.6. Additives as Promoters

3.1. Classification of Additives

3.5. Acidic Additives as Co-catalysts

3.2. Additives as Hydrogen Bonding Acceptors

3.3. Acidic Additives for Cationic Gold Catalyst

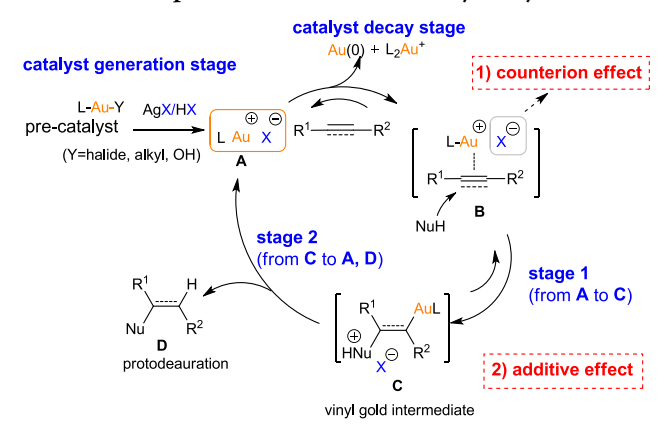
3.4. Acidic Additives for Cationic Gold Catalyst

on homogeneous gold catalysis.  $^{8-22}$  Cationic gold complexes are considered the most powerful catalysts for the electrophilic activation of unactivated multiple carbon—carbon bonds (alkynes, allenes, alkenes) due to their unique  $\pi$ -affinity. This superiority may be attributed to the lower LUMO and poor back-donation of the cationic gold species.  $^{23-26}$  The addition of a nucleophile to a gold activated alkyne/alkene/allene, either inter- or intramolecularly, provides diverse new chemical entities with high functional group compatibility and atom economy.  $^{8,9,11}$  In addition, gold catalysts are air and moisture tolerant. All these features have contributed substantially to the success of gold catalysis in organic synthesis.

Despite its unique advantages and versatile applications, gold catalysis still suffers from limitations such as low turnover numbers (TON) and turnover frequency (TOF). Many homogeneous gold-catalyzed reactions require relatively high catalyst loadings (1–5 mol %). To date, efficient gold catalysis with high TON and TOF is still limited.<sup>27–33</sup> This drawback has stimulated chemists to seek more efficient gold catalysts and to optimize reaction conditions.

A typical cationic gold catalytic cycle is illustrated in Scheme 1.<sup>34</sup> In stage 1, a cationic gold species A coordinates with an

Scheme 1. Simplified Cationic Gold Catalytic Cycle



unsaturated substrate such as an alkyne (or alkene),  $^{35}$  forming a  $\pi$ -gold-alkyne complex  $^{36-38}$  [L-Au-alkyne]X (B). B is subsequently attacked by a nucleophile (NuH) that results in the formation of a *trans*-alkenyl-gold complex (intermediate C) (nucleophile attack step). In stage 2, the reaction of C with an electrophile (E<sup>+</sup>) furnishes the final product D and regenerates the cationic gold catalyst A. The most common electrophile is proton (protodeauration). There are other processes or stages outside the catalytic cycle such as the on- and off-cycle process with the diaurated species.  $^{39-42}$  The formation of stable gemdiaurated intermediates may partly sequester the catalyst and hence slow down the reaction.  $^{43}$  A deactivation of the gold catalyst to nonreactive species (e.g., Au(0), or [L<sub>2</sub>Au]<sup>+</sup>) may occur in gold-catalyzed reactions (catalyst decay stage).

In most cases, the cationic gold catalyst A is not preformed but is generated *in situ* (catalyst generation stage). Well-defined cationic complexes have been first isolated and identified by Nolan<sup>44</sup> and then by others.<sup>45</sup> Silver salts AgX have been normally applied to activate the neutral LAuCl complexes through chloride abstraction for the *in situ* generation of cationic gold [LAu<sup>+</sup>]" (Scheme 1). However, those silver salts are not innocent in gold catalysis. Gagné and Weber<sup>46</sup> observed mixed Au—Ag intermediates as resting states of the gold catalysis. More

complicated Au-Ag-Au intermediates were also discovered by Jones. 47 Shi and co-workers 48 later demonstrated that Ag salts could influence the reaction rate and yield. The catalyst activation procedure could also affect gold catalysis efficiency. Echavarren<sup>49</sup> found that the order of addition of the silver salt can have a significant effect on reactivity as it may generate less active chloride-bridged dinuclear gold(I) complexes. Yu and coworkers<sup>50</sup> found that aquo- and oxo-gold complexes may form if water existed, and the insoluble silver salts were removed via Celite filtration. On the basis of the above studies, our group<sup>51</sup> proposed a practical protocol with a preformed LAu+Xcomplex generated by sonication followed by centrifugation. It could minimize the adverse silver effect and increase gold catalysis efficiency. Zhdanko and Maier<sup>52</sup> found that sliver may induce the off-cycle intermediates formation, which may cause the erratic silver effects.

Alternative ways without silver have also been developed. Teles and others<sup>5,53</sup> developed the Brønsted acid protonolysis of alkylgold. Nolan and co-workers<sup>54–58</sup> reported the Brønsted acid protonolysis of *N*-heterocyclic carbene (NHC) gold hydroxide to generated cationic gold species (Scheme 1).

### 1.2. Scope and Organization of the Review

Many factors may affect the four stages in gold-catalyzed reactions and therefore may decrease the efficiency of the overall reaction. First and foremost, the catalysis efficiency can be enhanced by fine-tuning the catalyst LAuX (A) itself through modifications of the ligand (L) and the counterion (X). In addition to the gold catalyst itself, reaction conditions, such as the use of additives, solvents, and even substrates, may affect the efficiency of reactions. Gold catalysis has experienced tremendous advances in the last two decades, as witnessed by the many reviews around this topic. 8–14,16–22,59 The ligand effect on gold catalysis has already been comprehensively investigated; 10,31,60,61 therefore, they will not be covered in this review. This review will focus on the effects of the counterion and additives in cationic gold-catalyzed reactions.

Bandini and co-workers published an excellent review of counterion effects in homogeneous gold catalysis in 2015; 62 therefore, we will concentrate on the counterion effects that have not been included in Bandini's review, that is, from late 2014 up to the present. To the best of our knowledge, there is no systematic review that summarizes the additive effects in gold catalysis. Therefore, it is necessary to cover the additive effects in a systematic fashion.

Our aim is to provide guidance to experimental organic chemists that want to optimize reaction conditions in cationic gold catalysis. This review is composed of counterion effect and additive effect in gold catalysis from a mechanistic perspective. Each section is subdivided by categories of the roles of counterion/additive exemplified with various gold-catalyzed reactions. Because of the intrinsic difficulty in finding the exact mechanistic role of counterions and additives, where often only empirical information has appeared in the literature, we organized this review based on our understanding of the reaction mechanism. To help readers follow the mechanistic pathway, we applied different colors for Au (gold color), counterions (blue color), and additives (pink color).

### 2. COUNTERION EFFECT

### 2.1. Classification of Counterions

Halides were the most employed counterions in the early stages of cationic gold catalysis. Particularly, Au(III) sources like

AuCl<sub>3</sub>, HAuCl<sub>4</sub>, and NaAuCl<sub>4</sub> were often used as these gold chlorides are more stable than the AuCl. However, this trend changed when new ligands and counterions in gold(I) catalysis appeared. As shown in Figure 1, commonly used counterions

Halides	O-based	N-based	C-based	B-based	Other fluorinated
X-	OR-	NR <sub>2</sub>	CR <sub>3</sub> -	BR <sub>4</sub>	MF <sub>n</sub> -
CI	OTs -	N(SO <sub>2</sub> Ph) <sub>2</sub>	CN-	BAr <sup>F</sup> 4	SbF <sub>6</sub> -
Br	OMs <sup>-</sup>	NTf <sub>2</sub>	HCTf <sub>2</sub>	BF <sub>4</sub>	PF <sub>6</sub> -
I٦	OTf <sup>-</sup>		CTf <sub>3</sub>	$B(C_6F_5)_4$	
	TFA-		TsC(CN) <sub>2</sub>	[Me <sub>3</sub> NB <sub>12</sub> C	111]
	CIO <sub>4</sub>				
	chiral Phosphate	)			

Figure 1. Common counterions in cationic gold catalysis.

can be categorized as halides, oxygen-based, nitrogen-based, carbon-based, boron-based, and other fluorinated counterions. Because of their relatively high stability and acceptable price,  $OTf^-$ ,  $SbF_6^{-,63-65}$   $NTf_2^-$  are the most common counterions used in cationic gold-catalyzed transformations.

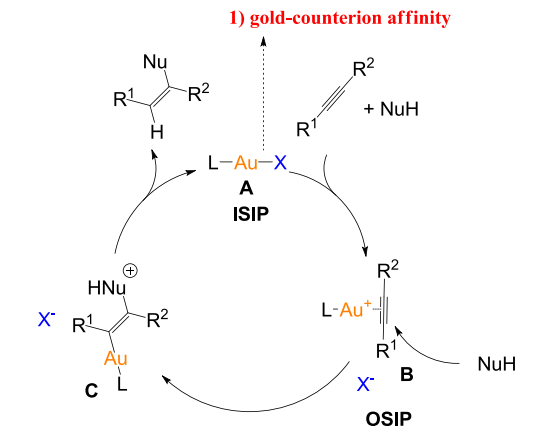
Cationic gold catalysis generally involves association/ dissociation processes surrounding the cationic gold center, counterion, or organic substrates. Solvents with different polarities play a distinct role in regulating this process. Generally, arenes (i.e., benzene, toluene) and halogenated solvents (i.e., DCM, DCE) with low dielectric constants are widely utilized in gold-catalyzed reactions, in which the gold catalyst exists as a contact ion pair.  $^{67-70}$  If the counterion is close to the reaction center, it could play an essential role in all stages of the reaction. 71 On the contrary, in polar solvents with high dielectric constants, like acetonitrile, nitromethane, and alcohols, cationic gold complexes may exist as dissociated ion pairs; cationic gold is heavily solvated. 67,72 As a result, counterions are relatively far away from the solvated cationic gold center and thus may have a smaller impact on the catalysis. Therefore, in this review, we will focus on the reactions conducted in low dielectric constant solvents, in which counterions do play a critical role. Furthermore, the presence of peculiar functional groups in the solvent could also affect the gold catalysis. 39,73-75 It may facilitate the nucleophilic attack or protodeauration steps. Also, it can compete with the alkyne/alkene substrates to coordinate with the cationic gold center, which affects the catalytic performances of the gold catalyst.

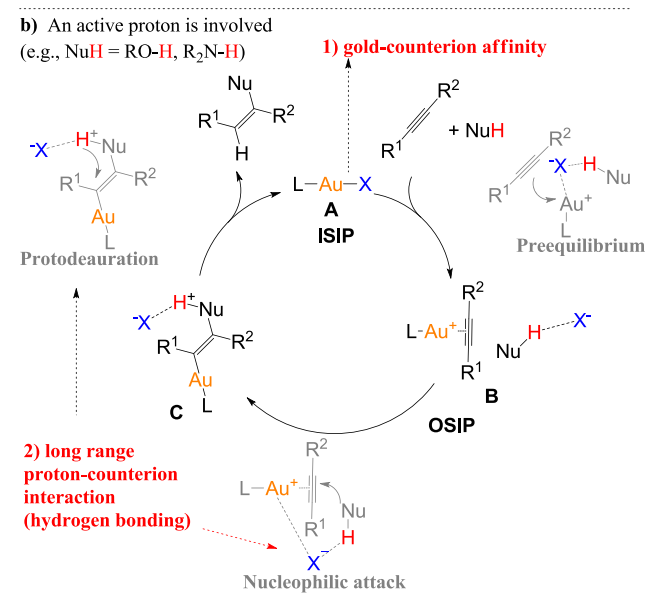
### 2.2. Physical Properties of Counterion Affecting Reactivities

Chemists have been interested in the physical properties of a counterion, in part, because they impact the catalytic activity, regioselectivity, and stereoselectivity of chemical reactions. <sup>43</sup> In general, the cationic gold catalyst **A** has to complex with an alkyne substrate in the catalytic cycle (from inner-sphere ion pair (ISIP) to outer-sphere ion pair (OSIP) in Scheme 2); the higher gold affinity of a counterion implies a higher energy barrier to overcome (Scheme 2). As a result, catalyst activity is generally inversely proportional to the gold affinity of the anion. In general, counterions (e.g., Cl<sup>-</sup>, OAc<sup>-</sup>) with high gold affinity will bind strongly with gold, preventing the coordination with the alkyne and therefore shutting down the catalytic cycle. <sup>76</sup> For gold-catalyzed reactions that do not involve an active proton, a cationic gold catalyst containing a weakly coordinating counter-

## Scheme 2. Counterion Effect in Cationic Gold Catalytic Circle

a) No active proton is involved (e.g., NuH = alkene)





**ISIP:** inner-sphere ion pair **OSIP:** outer-sphere ion pair

ion (low affinity between gold and counterion) will exhibit high reactivity (Scheme 2a).

However, for gold-catalyzed reactions that involve the transfer of an active proton (e.g.,  $O-H^{\delta+}$ ,  $N-H^{\delta+}$ ), gold affinity is not the only factor affecting the reaction (Scheme 2b). Because a proton has the smallest mass among all atoms, a counterion may exhibit a strong interaction with the active proton (Scheme 2b). In the nucleophile attacking step, the anion may act as a template and hold the nucleophile in the right position for the outer-sphere attack. As a hydrogen-bond acceptor, it will enhance the nucleophilicity of the attacking nucleophile. In the protodeauration step, the proton transfer often involves the activation/ cleavage of a heteroatom-H bond. The counterion can assist this process. The long-range interaction between an active proton and the counterion can be classified as a hydrogen bonding interaction, so the ability of a counterion to mediate the proton transfer could be quantified by its hydrogen bonding basicity. 77 In these cases, therefore, counterions possessing high hydrogen bonding basicity may play an essential role in the proton transfer. 78 However, it should be noted that counterions, as good hydrogen bond acceptors, may also have a high gold

affinity. Hence, the overall effectiveness of a counterion will depend on the delicate balance between its gold affinity and its hydrogen bond basicity. It should be noted that the existing states of cationic gold complexes (inner-sphere ion pair or outersphere ion pair) may play a critical role in the reactivity. L-Au-X likely exists as an inner-sphere ion pair, and its complexes with organic compounds such as alkynes, nucleophiles, or solvents may exist as outer-sphere ion pairs.

Moreover, counterions could affect gold catalyst stability. As shown in Figure 2, NTf<sub>2</sub><sup>-</sup> showed a more remarkable ability to

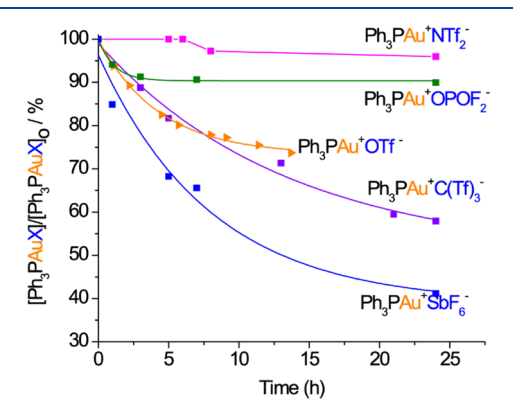


**Figure 2.** Decay of  $Ph_3PAu^+X^-$  in the presence of cyclohexene. Reproduced with permission from ref 74. Copyright 2014 John Wiley and Sons.

stabilize the gold catalyst in the presence of cyclohexene. This distinct stability with  $NTf_2^-$  was first demonstrated by Gagosz and co-workers. The deactivated gold catalysts include  $L_2Au^+$ , Au(0), and other unidentified gold species. However, the detailed role of counterion on the deactivation of gold catalysts is not clear yet. The existing states of cationic gold complexes (likely inner-sphere ion pairs) and their complex with cyclohexene (likely outer-sphere ion pairs) may play a critical role in the stability.

In addition, the anion/cation relative orientation could impact the catalytic performances of gold catalysts. If the anion is forced away from the catalytic site through the hydrogen bonding interaction of the auxiliary ligand with the anion, the reaction will slow down. Conversely, if the anion is located near the alkyne, the reaction will be assisted.<sup>79</sup> Macchioni and Zuccacia 68,80-82 made excellent contributions on the rationalization of ion-pairing structures in phosphine- and carbenebased cationic gold complexes with alkenes/alkyne substrates. With NOE NMR spectroscopy and DFT calculations, they found that the exact position of the counterion is determined by the electronic and steric properties of the ancillary ligand and substrate. The counterion is located on the substrate side in the complexes with poorly electron-donating phosphine ligands (see B3 in Figure 3). While for the complexes with good electron-donating NHC ligands, the counterion preferred to stay next to the ligand (see B1 in Figure 3). In many cases, the catalytic efficiency of a given L-Au-X species should not only be



 $(L=Phospine\ ligand\ /\ NHC\ ligand;\ X^{-}=Weakly\ coordinating\ counterion;\ S=alkenes\ /\ alkynes)$ 

Figure 3. Three types of gold cation/counterion orientations.

evaluated by the properties of L and  $X^-$  separately. Zuccaccia<sup>83</sup> first pointed out ligand and counterion must be considered simultaneously, which was further emphasized later by Hashmi's group. <sup>84,85</sup> The appropriate matching of  $X^-$  and the neutral ligand could affect the catalytic performance of gold catalysts. <sup>21</sup>

Nolan and co-workers synthesized stable gold species in the presence of a tetrafluoroborate counterion  $[Au(IPr^{Cl})(FBF_3)]/[Au(IPr^{Cl})(L)][BF_4]$  (Scheme 3, compound 2) using methods

# Scheme 3. Experimental Evidence for Inner-Sphere versus Outer-Sphere Coordination of BF<sub>4</sub><sup>-</sup> in Complex 2

A or B (avoiding silver salts). IR and X-ray studies described complex 2 in the solid-state as an inner-sphere complex. Although complex 2 was bench stable, in solution, a dynamic equilibrium between two conformations was found with the counterion occupying inner-sphere (2) and outer-sphere (4) positions based on studies of NMR, stoichiometric reactivity, and catalytic activity. Also, computational modeling further revealed the interconversion between inner-sphere and outersphere coordinating counterions and the favorable coordination of solvent molecules in the gold complex with an empty coordination site, where the BF4- anion resided in the outer sphere.<sup>86</sup> Pulsed-field gradient (PFG) NMR and its implementation DOSY (diffusion-ordered NMR spectroscopy) are useful techniques for the investigation of interactions between substrates and to characterize reactive intermediates. Together with external calibration curves (ECC), Dumez and coworkers<sup>87</sup> could obtain substantial interaction evidence between cationic gold(I) and their counterion or the substrate. This may help to rationalize the reactivity of reagents in gold-catalyzed reactions.

# 2.3. Gold Affinity and Proton-Affinity and Hydrogen Bond Basicity Scale of Counterions

As stated earlier, the gold affinity and hydrogen bonding basicity of counterions may play critical roles in gold-catalyzed reactions. Therefore, a quantitative description of the gold affinity and hydrogen-bond basicity of counterions is beneficial. Ujaque and co-workers reported the gold affinity data through the calculation of the dissociation energy of several PPh<sub>3</sub>AuX complexes into the corresponding cationic [PPh<sub>3</sub>Au<sup>+</sup>] and anion X<sup>-</sup> in dichloromethane (Figure 4). The calculations showed that the gold affinity of different counterion follows the following trend:  $CF_3CO_2^- \approx Cl^- > NO_3^- > OTs^- > OTf^- > BF_4^-$ . Later, Zhdanko and Maier reported a gold affinity scale of various

LAuX	D0	CE -	LAu <sup>+</sup>	+ X-		
L	OTf <sup>-</sup>	NO <sub>3</sub>	CI	TsO	CF <sub>3</sub> COO <sup>-</sup>	BF <sub>4</sub>
PH <sub>3</sub>	0.0	11.0	12.3	7.1	13.0	-4.3
PPh <sub>3</sub>	0.0	8.2	12.5	6.3	13.2	-2.3
The energy reaction of PAuOTf is defined as zero.						

**Figure 4.** Relative metal—ligand (LAuX) dissociation energies in dichloromethane. Reproduced with permission from ref 88. Copyright 2008 American Chemical Society.

counterions based on  $^1\text{H}$  and  $^{31}\text{P}$  NMR spectroscopy (Figure 5, NMRs could be found in the references). Both scales showed that  $\text{OTf}^-$  and  $\text{NTf}_2^-$  have a moderate gold affinity, and  $\text{OTs}^-$  has the highest gold affinity.

**Figure 5.** Gold affinity scale of counterions was established based on experimental ligand exchange equilibria in CD<sub>2</sub>Cl<sub>2</sub>. Reproduced with permission from ref 89. Copyright 2014 American Chemical Society.

Although these pioneering works on the gold affinity of counterions are highly useful, data for some commonly used counterions were not included. With more counterions being utilized in gold catalysis, our group established a relatively comprehensive scale, namely, a counterion gold affinity index (GAI), using the calculated dissociation energy. GAI ranges from 0 to 10, where a bigger number indicates a higher affinity to gold (Table 1).

Table 1. Gold Affinity Index of Counterions

$$L-Au-X$$
  $\xrightarrow{DCM}$   $L-Au$  +  $X$   $(L = Me_3P)$ 

counterion	dissociation energy $\Delta E$ (kJ/mol)	gold affinity index (GAI)
I <sup>-</sup>	143.8	10
Br <sup>-</sup>	67.7	6.0
Cl <sup>-</sup>	53.9	5.2
TFA <sup>-</sup>	74	6.3
OAc <sup>-</sup>	70.6	6.1
OTs <sup>-</sup>	28	3.8
$\mathrm{NTf_2}^-$	10.4	2.9
OTf <sup>-</sup>	0	2.4
BF <sub>4</sub> <sup>-</sup>	-35.1	0.5
CTf <sub>3</sub> <sup>-</sup>	-40.5	0.2
SbF <sub>6</sub>	-44.3	0
$Al[OC(CF_3)_3]_4^-$	<-45	<0
BArF <sub>4</sub>	<-45 <-45	<0

Although experimental data for hydrogen bonding basicity of counterions (e.g., Lawrence and co-workers'  $pK_{BHX}$ )<sup>92</sup> are available, just as they were for the gold affinity index, data for many common counterions were not available. We established a hydrogen bond basicity index of common counterions based on calculated data of the hydrogen bonding energies of various

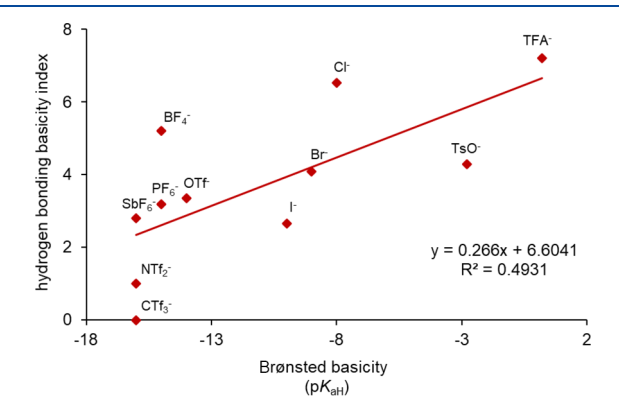
counterions with phenol (Table 2). This index also ranges from 0 to 10, where a bigger number indicates a higher affinity to the proton (or higher hydrogen bond basicity).

Table 2. Hydrogen Bond Basicity Index of Counterions

$$Ph \xrightarrow{O} H + X^{\bigcirc} \longrightarrow Ph \xrightarrow{O} H \xrightarrow{X^{\bigcirc}} \Delta E = (E_1 + E_2) - E_3$$

(X <sup>-</sup> )	$pK_{aH}$	hydrogen bonding energy $(\Delta E) \Delta E \text{ (kJ/mol)}$	hydrogen bond basicity index (HBI)
OAc <sup>-</sup>	4.7	149.7	10
$TFA^-$	0.2	122.1	7.2
$TsO^-$	-2.8	93.1	4.3
Cl <sup>-</sup>	-8	115.3	6.5
$Br^-$	-9	91.1	4.1
I <sup>-</sup>	-10	76.9	2.6
OTf	-14	83.9	3.4
$PF_6^-$	<-10	82.2	3.2
$\mathrm{BF_4}^-$	<-10	102.2	5.2
SbF <sub>6</sub>	<-10	78.5	2.8
$NTf_2^{-}$	<-10	60.6	1.0
CTf <sub>3</sub> <sup>-</sup>	<-10	50.7	0

It should be noted that the hydrogen bonding basicity and Brønsted basicity of counterions have a poor correlation (Figure 6).<sup>91</sup> This means that a strong hydrogen bonding acceptor is not



**Figure 6.** Lack of good correlation between Brønsted basicity ( $pK_{aH}$ ) and hydrogen bonding basicity index. Reproduced with permission from ref 91. Copyright 2017 American Chemical Society.

necessarily a strong Brønsted base. Although Brønsted basicity of counterions could be used as an indicator for the ability to assist proton transfer, our group found that hydrogen bonding basicity is often a more accurate indicator for the proton transfer process (Scheme 2b). Besides, the hydrogen bonding basicity and the gold affinity index of counterions also have a poor correlation.

## 2.4. Counterion Effects on Reactivity and Chemo-/Regioselectivity

**2.4.1. Effect of Counterions on Reactivity.** The gold affinity indexes could be used to rationalize the counterions' kinetic effects in gold-catalyzed reactions (Table 3). For reactions in which no active proton is involved (e.g., cycloisomerization of 1,6-enyne 5, Table 3), a gold catalyst with low gold affinity counterions (e.g.,  $Al[OC(CF_3)_3]_4^-$ ) showed faster kinetics.

Table 3. Gold Affinity-Related Counterion Effect on Cycloisomerization of 1,6-Enyne

In gold-catalyzed reactions involving active proton transfer, the hydrogen bonding basicity of counterions may play a critical role. The hydrogen bonding basicity index in the gold-catalyzed cyclization of propargyl amide allowed us to rationalize the kinetic effects of counterions (Table 4). 91 For reactions in which

Table 4. Hydrogen Bonding Basicity-Related Counterion Effect on Cyclization of Propargyl Amide

X-	hydrogen bonding basicity index (HBI)	relative initial rate
OAc <sup>-</sup>	10	0.0
OTf	3.4	5.1
$NTf_2^-$	1.0	0.9
SbF <sub>6</sub> <sup>-</sup> CTf <sub>3</sub> <sup>-</sup>	2.8	1.0
$\mathrm{CTf_3}^-$	0	1.0

protodeauration is the rate-limiting step (e.g., cyclization of propargyl amide 7, Table 4), a counterion with high hydrogen bond basicity (e.g., OTf<sup>-</sup>) assisted the proton transfer and spedup the reaction. As we discussed above, counterions could deactivate the gold catalyst through their strong gold affinity, preventing the coordination with the alkyne (see OAc<sup>-</sup> in Table 4, GAI = 6.1).

The Bandini group developed a regioselective and stereoselective dearomatization of substituted 2-naphthols with allenamides catalyzed by PPh<sub>3</sub>AuTFA (Scheme 4). They proposed a synergistic  $\pi$ -acid ([PPh<sub>3</sub>Au]<sup>+</sup>) and Lewis base

# Scheme 4. PPh<sub>3</sub>AuTFA Catalyzed Dearomatization of Substituted 2-Naphthols

(TFA<sup>-</sup>) catalysis to explain the experimental results. The simultaneous electrophilic activation on the allenyl core by cationic gold and the basic TFA<sup>-</sup> (p $K_a$  = 0, HBI = 7.2) activating/directing effect on naphthol ensured the optimal electron/space arrangement for the C–C bond formation (Scheme 4). Other gold catalsyts with different counterions (AcO<sup>-</sup>, SbF<sub>6</sub><sup>-</sup>, OPNB<sup>-</sup>, OTf<sup>-</sup>, and OTs<sup>-</sup>) were tested without success. AcO<sup>-</sup>, OPNB<sup>-</sup>, and OTs<sup>-</sup> with high gold affinity are not substituted by the allenamide and thus the reaction cannot start. While SbF<sub>6</sub><sup>-</sup>, OTf<sup>-</sup> with poor hydrogen bonding basicity caused allenyl unit decomposition. Only TFA<sup>-</sup> with appropriate compromise between metal-coordination ability and hydrogen bond basicity gave satisfactory results (see intermediate 13 in Scheme 4). <sup>93</sup>

Zhdanko and Maier found that the hydrogen bonding ability of counterions also played a vital role in the gold-catalyzed addition of an alcohol to an alkyne (Figure 7). 89,90

ion pair AX

By hydrogen bonding with ROH, X enhances nucleophilicity of ROH in order:  $SbF_6^- < NTf_2^- < ClO_4^- < OTf^- < OTs^-$ 

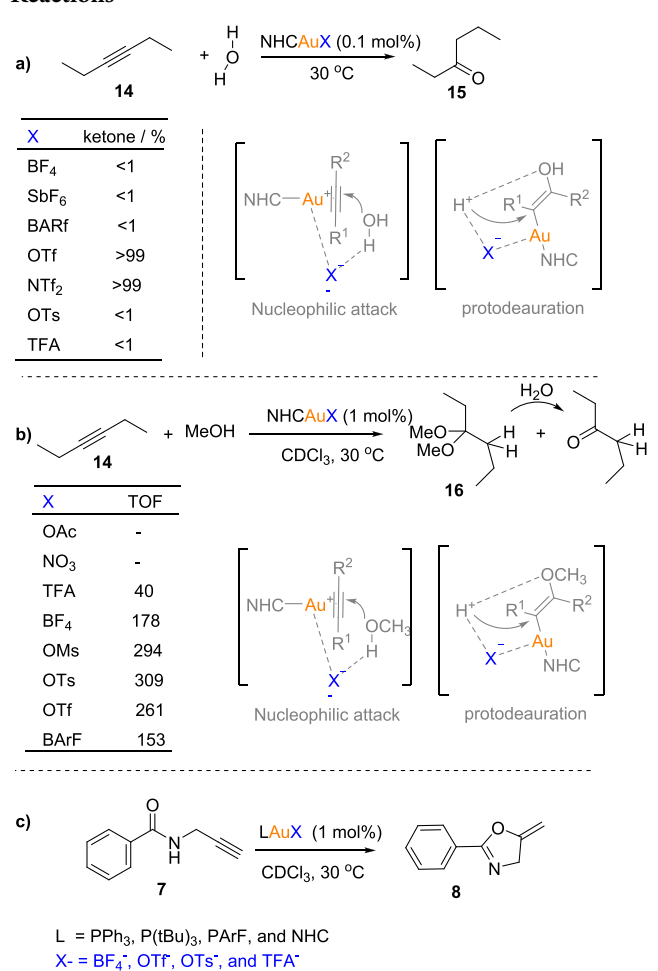
**Figure 7.** Counterion effects by hydrogen bonding with ROH. Reproduced with permission from ref 89. Copyright 2014 American Chemical Society.

Zuccaccia and co-workers in 2016 investigated the activity of different NHCAuX ((NHC = 1,3-bis(2,6-diisopropylphenyl) imidazol-2-ylidene, X = BArF<sup>-</sup>, BF<sub>4</sub><sup>-</sup>, SbF<sub>6</sub><sup>-</sup>, OTf<sup>-</sup>, NTf<sub>2</sub><sup>-</sup>, ClO<sub>4</sub><sup>-</sup>, OTs<sup>-</sup>, TFA<sup>-</sup>) in the sustainable hydration of an alkyne under solvent-, silver-, and acid-free conditions (Scheme 5a). The counterions played vital roles that were rationalized by kinetic experiments and DFT calculations. Of all the coordinating ions considered, OTf<sup>-</sup> and NTf<sub>2</sub><sup>-</sup> assisted the reactions due to the ideal balance of their gold coordinating ability and basicity. Secondary of the coordinating ability and basicity.

The same group also used the counterion effect on the gold-catalyzed alkoxylation of alkynes (Scheme 5b). The effect of the counterion depends on both its intrinsic properties (basicity, coordinating power, and even geometry) and its correlation with the nucleophile. A counterion plays a vital role in all steps of the reaction mechanism: pre-equilibrium, nucleophilic attack, and protodeauration (Scheme 2b). In particular, NTf2-, OTf-, OTs-, and OMs- promoted the nucleophilic attack owing to their basicity. However, strongly coordinating counterions (e.g., NO3-, OAc-) slowed down or inhibited the reaction (ISIP  $\leftrightarrows$  OSIP, equilibrium in favor of ISIP) (Scheme 5b).

The ligand and counterion also showed a combined effect in gold(I)-catalyzed alkoxylation of alkynes. Belanzoni and coworkers compared the gold catalysis with  $P(fBu)_3/NHC$  ligand and various counterions. They found that the catalytic efficiency depends on the anion/ligand interplay, which played an important role in the nucleophilic attack step of the reaction mechanism. With a charge-displacement analysis, they discovered that the unsaturated multiple bonds activation (alkyne) by the cationic gold catalyst depends on the counterion affinity for the cationic fragment and the ligand-withdrawing ability at the outer region of the C-C bond. Without the anion, gold catalysts with NHC and  $P(fBu)_3$  owned the same ability for substrate

## Scheme 5. Counterion Effects on Common Gold-Catalyzed Reactions



activation. While in the presence of OTs<sup>-</sup>, the counterion could affect the transition state of the nucleophilic attack and offset the ligand effect. Because the OTs<sup>-</sup> counterion is closer to  $P(tBu)_3$ , the gold is less inclined to accept electronic density from the alkyne substrates, which makes the activated alkyne less electrophilic for the nucleophilic attack.

The same group further investigated the combined effects of a ligand and a counterion on the cycloisomerization of N-(prop-2ynyl)benzamide 7 (Scheme 5c) and the methoxylation of 3hexyne 14 (Scheme 5b). In reaction c, the RDS (ratedetermining step) is protodeauration, noncoordinating, and weakly basic anions (such as  $BF_4^-$ ) performed best with the NHC ligand. While in reaction b, the RDS is the counterion assisted nucleophilic attack; consequently, OTs performed best with the NHC ligand because of its intermediate coordinating ability, basicity, and hydrogen bond acceptor properties. When a phosphine ligand was tested, the result turned out to be completely different. In reaction c, relatively high basicity and hydrogen bond acceptor properties (OTs and TFA) promoted the cycloisomerization, whereas in reaction b, low coordinating and a weakly basic counterion (BF<sub>4</sub><sup>-</sup> and OTf<sup>-</sup>) was the better choice. We believe that the reason for this behavior is that, in the phosphine case, the higher affinity of the counterion (such as OTs<sup>-</sup>) toward gold stimulates the reaction when the RDS is the protodeauration step but inhibits it when the RDS is the nucleophilic attack (the equilibrium is shifted toward the ISIP).83

### 2.4.2. Effect of Counterions on Chemo-/Regioselectiv-

**ity.** For a gold-catalyzed reaction that encompasses the transfer of a proton, in addition to reaction kinetics, a gold catalyst containing a counterion with high hydrogen bond basicity may significantly impact the chemo-/regioselectivity of the reaction.

You and co-workers investigated the intramolecular dearomatization of 1-naphthol 17 with gold complex Ph<sub>3</sub>PAuCl and various chloride scavengers (Scheme 6).<sup>96</sup> When the relatively

# Scheme 6. Counterion Effect on Gold-Catalyzed Intramolecular Dearomatization of 1-Naphthol

Ph<sub>3</sub>PAuX

pathway A

$$X = OMs^{-}$$

pathway B

Ph<sub>3</sub>PAuX

 $X = OMs^{-}$ 
 $X = O$ 

basic counter anion MsO was employed, the 5-endo-dig cyclization was facilitated by the concomitant deprotonation promoted by counterion MsO<sup>-</sup> furnishing the spirocyclic gold intermediate 22, which then formed the spirocarbocyclic product 18. Alternatively, this cyclization might have followed the typical 1,5-enyne cycloisomerization route to form a cyclopropyl gold carbene 21, which might then undergo MsO- promoted deprotonative fragmentation to give the same intermediate 22. When the less basic NTf<sub>2</sub><sup>-</sup> was utilized, the fragmentation of the bold bond of the cyclopropane ring in intermediate 21 was preferred over the depicted deprotonative fragmentation, affording, in turn, the product 19. This experimental outcome could be rationalized quantitatively, invoking the higher hydrogen basicity of OMs (hydrogen bond basicity index is around 4.3) compared to NTf<sub>2</sub><sup>-</sup> (hydrogen bond basicity index = 1.0, see Table 2).

Gevorgyan and co-workers developed two Au-catalyzed protocols, where depending on the choice of ligand and counterion, regioisomeric boryl furans can be selectively synthesized (Schemes 7, 24a, and 24b). They proposed a tentative  $\pi$ -activation mechanism (pathway A) and an alternative  $\sigma$ -activation mechanism (pathway B) shown in Scheme 7. Zhang and co-workers further pursued the mechanism of this reaction with a theoretical study. The results revealed that the reaction underwent  $\sigma$ -activation of the oxirane moiety (pathway B) rather than  $\pi$ -activation of an alkynyl moiety (pathway A). This is contrary to the proposed mechanism in the experimental work. The mechanism comprises two major stages: alkynyloxirane ring expansion and 1,2-B or 1,2-H migration toward divergent borylated furans. The counterion and ligand are less critical for the oxirane ring expansion but are both crucial to the divergent formation of

# Scheme 7. Catalytic Cycles for Regiodivergent Gold(I)-Catalyzed Cycloisomerization of Alkynyl Oxirane

borylated furans. The Gibbs free energy barriers for the 1,2-H migrations and 1,2-B migrations were calculated for catalysts with different counterions. They found that more basic OTfcounterion favored 1,2-H migrations pathway and less basic SbF<sub>6</sub> counterion favored 1,2-B migrations pathway. They also found that the barriers of 1,2-B migration processes are comparable for the two catalysts (12.0 kcal/mol for (2,4-ditBuO)<sub>3</sub>PAuOTf vs 11.0 kcal/mol IPrAuSbF<sub>6</sub>). However, the barriers of 1,2-H migration processes are significantly different for the two catalysts (8.9 kcal/mol for (2,4-di-tBuO)<sub>3</sub>PAuOTf vs 19.3 kcal/mol IPrAuSbF<sub>6</sub>). Therefore, they assumed that such a large barrier difference (10.4 kcal/mol) originated not only the counterion effect but also the ligand effect. C3-borylated furan 24a was formed by 1,2-H migration with the relatively more basic OTf counterion and (2,4-di-tBuO)<sub>3</sub>P ligand, whereas C2borylated furan 24b was the favored product when using  $Sb\overline{F_6}$ counterion with IPr ligand through 1,2-B migration.9

Van der Eycken and co-workers investigated a post-Ugi gold(I)-catalyzed domino dearomatization/ipso-cyclization/ aza-Michael sequence. 99 In particular, the tetracyclic reaction from 29 afforded 30 when catalyzed by PPh<sub>3</sub>AuCl/AgNTf<sub>2</sub>, and 31 when catalyzed by AuPPh<sub>3</sub>Cl/AgOTf. Furthermore, the spirocarbocyclic product 30 proved to be an intermediate of the domino cyclization by employing 30 in AuPPh<sub>3</sub>Cl/AgOTf to yield 31 at 99% (Scheme 8a). Recently, Zhao and Li unraveled the mechanism of this reaction in detail with a DFT study (Scheme 8b). The crucial role of counterions was shown in two separate steps: the dearomatizing spirocyclization via a hydrogen bond bridge (32 to 33) and the aza-Michael addition (34 to 35). In the aza-Michael addition step, the gold affinity of counterion X<sup>-</sup> controls the coordination mode of 34, which in turn controls its reactivity. If the NTf2- counterion, which has relatively high gold affinity and low hydrogen bonding basicity, is used, the aza-Michael addition reaction is inhibited and the spiro carbocyclic intermediate 30 is obtained.<sup>10</sup>

### Scheme 8. Gold-Catalyzed Domino Cyclization

The counterion influence on the gold intermediates, generated during the gold-catalyzed intramolecular hydroalkoxylation of allenes, was reported by Widenhoefer and coworkers (Scheme 9). In the reaction of allene 36 with

# Scheme 9. LAuCl/AgOTs and LAuCl/AgSbF<sub>6</sub> Catalyzed Intramolecular Hydroalkoxylation of Allene

(a) Ph OH 
$$\frac{\text{LAuCl/AgOTs}}{\text{CD}_2\text{Cl}_2, -60 \, ^{\circ}\text{C}}$$
 Ph OH  $\frac{\text{AuL}}{\text{CD}_2\text{Cl}_2, -60 \, ^{\circ}\text{C}}$  Ph OH  $\frac{\text{AuL}}{\text{CD}_2\text{Cl}_2, -60 \, ^{\circ}\text{C}}$   $\frac{\text{AuL}}{\text{CD}_2\text{Cl}_2, -80 \, ^{\circ}\text{C}}$   $\frac{\text{AuL}}{\text{CD}_2\text{Cl}_2, -80 \, ^{\circ}\text{C}}$   $\frac{\text{Cl equiv}}{\text{CD}_2\text{Cl}_2, -80 \, ^{\circ}\text{C}}$   $\frac{\text{Cl equiv}}{\text{Cl}_2\text{Cl}_2, -78 \, ^{\circ}\text{C}}$   $\frac{\text{Cl}_2\text{Cl}_2, -78 \, ^{\circ}\text{C}}{\text{Cl}_2\text{Cl}_2, -78 \, ^{\circ}\text{C}}$   $\frac{\text{Cl}_2\text{Cl}_2, -78 \, ^{\circ}\text{Cl}}{\text{Cl}_2\text{Cl}_2, -78 \, ^{\circ}\text{C}}$   $\frac{\text{Cl}_2\text{Cl}_2, -78 \, ^{\circ}\text{Cl}}{\text{Cl}_2\text{Cl}_2, -78 \, ^{\circ}\text{Cl}_2}$   $\frac{\text{Cl}_2\text{Cl}_2, -78 \, ^{\circ}\text{Cl}_2}{\text{Cl}_2, -78 \, ^{\circ}\text{Cl}_2}}$   $\frac{\text{Cl}_2\text{Cl}_2, -78 \, ^{\circ}\text{Cl}_2}{\text{Cl}_2, -78 \, ^{\circ}\text{Cl}_2}}$   $\frac{\text{Cl}_2\text{Cl}_2, -78 \, ^{\circ}\text{Cl}_2}{\text{Cl}_2, -78 \, ^{\circ}\text{Cl$ 

JohnPhosAuCl/AgOTs, the irreversible C-O bond formation delivered the mono(gold) vinyl complex 39, which went through rapid auration to afford the bis(gold) vinyl complex 37 followed by protodeauration to give the product 38 (Scheme 9a). On the other hand, in the reaction of 36 with JohnPhosAuCl/AgSbF<sub>6</sub>, the  $\pi$ -coordinated vinyl tetrahydropyran complex 40 was formed via rate-limiting C-O bond formation followed by rapid protodeauration instead of auration (Scheme 9b). 101 The different outcome with the two counterions was attributed to the lower gold affinity of SbF<sub>6</sub><sup>-</sup> than OTs<sup>-</sup>. As proved by the formation of the gold complex **36a** early and the gold complex 40 later in the reaction of 36 with JohnPhosAuCl/AgSbF<sub>6</sub> (Scheme 9b). Meanwhile, the fast formation of the gold  $\pi$ -allene complex 36a instead of the bis(gold) vinyl complex 37 indicates rate-limiting C-O bond formation in the reaction with JohnPhosAuCl/AgSbF<sub>6</sub>. The

hydrogen bonding basicity disparity of the two counterions also accounts for the reaction divergence. Despite a much higher concentration of the reactive gold complex 36a in the reaction with JohnPhosAuCl/AgSbF<sub>6</sub>, the C–O bond formation was not faster than the case with JohnPhosAuCl/AgOTs. This could be explained by the higher hydrogen bonding basicity of OTs<sup>-</sup> than SbF<sub>6</sub><sup>-</sup>, which assisted the deprotonation process for the C–O bond formation in the reaction with JohnPhosAuCl/AgOTs.

Occhiato and co-workers investigated the gold(I)-catalyzed propargyl Claisen rearrangement/Nazarov cyclization of propargyl vinyl ether derivatives. Different counterions were considered in their study. In particular, when using Ph<sub>3</sub>PAuSbF<sub>6</sub> (Scheme 10, top), the reaction was completed in 1 h and

Scheme 10. Catalytic Cycle of Gold(I)-Catalyzed Propargyl Claisen Rearrangement/Nazarov Cyclization of Propargyl Vinyl Ether Derivatives

afforded the target compound **42a** as the major product (74%); with  $\mathrm{BF_4}^-$  as the counterion, the reaction was sluggish and was still incomplete after 5 h, affording a mixture containing the starting materials (Scheme 10, top). Using  $\mathrm{OTf}^-$  as the counterion (Scheme 10, top), the reaction was much faster (0.5 h) and yielded **42a** only. The proposed catalytic cycle is shown in Scheme 10. It should be noted that the process undergoes a [1,2]-H shift from position 5 to 6 in intermediate **43** to generate cation **44**. The control experiment suggests that the deprotonation at C5 is followed by protodeauration. Compared with other counterions examined in this study, the better performance of  $\mathrm{OTf}^-$  could be attributed to its greater basicity.  $^{102}$ 

420

The proximity of a counterion to a charged catalyst in an ion paired complex gives rise to strong electrostatic interactions, which can alter the regioselectivity of intramolecular hydroarylation to afford 2*H*-chromenes. A case in point is Kanan and co-workers' study on the gold-catalyzed intramolecular hydroarylation (Scheme 11) to produce 5-substituted 2*H*-chromene

Scheme 11. Regioselectivity of Intramolecular Hydroarylation

46a and 7-substituted 2H-chromene 46b.  $^{103}$  When this group used the large counterion  $B(Ar^F)_4$ , the energies of unpaired transition states showed very little  $\varepsilon$  (dielectric constant)-dependence. Similar regioselectivity results (46a:46b = 1:0.7) were observed when  $\varepsilon$  increased from 2.4 to 11.4. In contrast, if ion-pairing was preserved after the interaction between the ion pair and the dielectric medium, the energy difference of ion paired transition states diminished rapidly with increasing  $\varepsilon$ . Notably, when this group used a small counterion,  $SbF_6^-$ , the regioselectivity changed (from 1:0.8 to 1:5) when  $\varepsilon$  decreased from 11.4 to 2.4.

Yang and Fang performed density functional theory (DFT) calculations to probe the chemoselectivity of *o*-(alkynyl)styrene 47 containing an isopropyl and methyl groups at the terminal position of an alkene (Scheme 12). The chemoselectivity was

Scheme 12. Counterion Effect on Gold-Catalyzed Cycloisomerization of o-(Phenylethynyl)styrene

mainly controlled by the electronic effect of the counterion and the substituent. In the presence of the counterion  ${\rm SbF_6}^-$ , the reaction was more prone to promote a 1,2-H shift (isopropyl H) than elimination, affording ring expansion product 49a. However, in the presence of the more basic  ${\rm OTs}^-$ , proton elimination was mainly observed, affording the indenyl derivative 49b.  $^{104}$ 

In 2018, the Hashmi group, inspired by Biasiolo et al.,<sup>83</sup> conducted a broad screening of key parameters in typical reactions in homogeneous gold catalysis. The result of this study

I

indicated that there was a more pronounced counterion influence in the reaction outcome compared to the ligand, which meant that the best counterion for a given gold-catalyzed reaction also exhibited the highest activity with every other ligand investigated in that particular reaction. For example, in a cyclopropanation reaction (Scheme 13, eqs 1 and 2), the

# Scheme 13. Tested Reactions Concerning the Ligand and the Counterion of Gold Catalysts

counterion NTf<sub>2</sub><sup>-</sup>, in combination with one of three typical ligands (IPr, PPh<sub>3</sub>, and SPhos) performed best. This observation simplified the screening procedure because, in the first screening, they only needed to examine a large number of various counterions using a limited set of ligands (IPr, PPh<sub>3</sub>, and SPhos) to tease out the best counterion. In a second screening, they subsequently investigated a large variety of ligands in combination with the superior counterion found in the first screening step to identify the ideal gold catalyst (Scheme 13a). For the remaining reactions studied by the Hashmi group, including the rearrangement of an allenyl ether (eq 3), oxidative gold catalysis using N-oxides (eq 4), hydroarylation (eq 5), and the synthesis of an alkylideneoxazoline (eq 6), the same procedure was applied to tease out the optimal gold catalyst.<sup>84</sup> They also investigated counteranions Pathal,  $B(CN)_4$ , TFA,  $(BAr^{F_4})^{-}$ ,  $[B(C_6F_5)_4]^{-}$ ,  $Al[OC(CF_3)_3]_4^{-}$ , and  $[B-1]_4^{-}$ (C<sub>6</sub>F<sub>5</sub>)<sub>3</sub>(OAc<sup>F</sup>)]<sup>-</sup>, which are generally overlooked but can sometimes surpass or at least match common counterions in terms of catalytic activity (Scheme 13b). For example, in the synthesis of an alkylideneoxazoline (eq 6), OTs-, TFA-, and  $[B(C_6F_5)_3(OAc^F)]^-$  gave the best results because of their strong coordinating ability and excellent proton acceptor capacity due to the fact that the transition-state intermediate contained an active proton (-NH).85

1,6-Allenynes **62** can be converted to very distinct products in a highly selective fashion under various noble-metal catalysis.

After a thorough investigation of various factors like ligand, counterion, and metal catalyst, Fensterbank and co-workers proposed a refined mechanism, which well explained the divergent reactivities. <sup>105</sup> As shown in Scheme 14, one pathway

# Scheme 14. Mechanistic Pathways for Divergent Gold-Catalyzed Cycloisomerization of 1,6-Allenynes

involves a 1,4-hydride shift process that follows a C(sp³)-H insertion to the gold vinylidene intermediate 64, and it afforded a hydrindiene product 65. The other pathway produced a classical Alder-ene cycloisomerization product 67, which goes through a 1,5-proton shift process. Counterions like OTf⁻ could serve as a proton shuttle to assist this process and thus favor this pathway.

# 2.5. Additional Computational Studies on the Role of Counterion as Hydrogen Bond Acceptors

Miscione and co-workers reported a computational DFT investigation on the mechanism of the last stage reaction (69 to 70) in the synthesis of azepino-indole 70 catalyzed by [Au(IPr)Cl]/AgOTf. The gold catalyst activated the substrate through the formation of a carbon–gold  $\sigma$  complex, which acted as a nucleophilic alkenyl-gold species (intermediate 71, Scheme 15). OTf played crucial roles in all steps of the reaction mechanism. Especially, in the ring-closing step (intermediate 69 to intermediate 72, Scheme 15), it activated the carbonyl group C3–O4 (Scheme 15, 71). The  $\sigma$ -bonded gold atom favored pathway a because the structure of intermediate 73 was flexible enough to allow a significant decrease of the C1···C4 distance, facilitating the H3 transfer (Scheme 15).

Li and co-workers shed light on the effect of counterion on the Au(I)-catalyzed synthesis of dihydrocyclopentylindole derivative 75 from indole-allenoate 74, also using DFT calculations (Scheme 16). The reaction mechanism included three essential processes: the intramolecular cyclization (74 to 77) and the subsequent two-step proton transfer process (77 to 78 and 79 to 80). Their calculation showed that counterions not only can serve as hydrogen bonding acceptors to assist the intramolecular cyclization but also can significantly reduce the energy barrier of the proton transfer process. In the two-step proton transfer process, the selected counterions BF<sub>4</sub>, OTf, and Cl showed a reversed catalytic activity order. In the step of the counterion protonation (77 to 78), the catalytic activity of the counterion increased in the order: BF<sub>4</sub><sup>-</sup> < OTf<sup>-</sup> < Cl<sup>-</sup>, which affected the proton transfer process from C5 to the counterion. However, in the deprotonation of counterion-H (79 to 80), the sequential order of the catalytic ability was Cl<sup>-</sup> < OTf<sup>-</sup> < BF<sub>4</sub><sup>-</sup>, which influenced the proton migration from the counterion to C2. The OTf with appropriate hydrogen bonding basicity showed a moderate catalytic ability in both steps, and the (PPh<sub>3</sub>)AuOTf

Scheme 15. Mechanism of Last Stage in Synthesis of Azepino-Indole Catalyzed by [Au(IPr)Cl]/AgOTf

was found to have the lowest free energy barriers in the intramolecular cyclization as the rate-determining step. Therefore,  $(PPh_3)AuOTf$  is more favorable than  $(PPh_3)AuCl$  and  $(PPh_3)AuBF_4$  for this reaction.  $^{107}$ 

### 2.6. Chiral Counterion Enabled Asymmetric Reactions

Although Au(I) catalyzed enantioselective transformations involving chiral ligands bound to the gold metal center have been widely successful, this strategy has had its own downside. First, a very common issue is the tendency of gold(I) to form linear two-coordinate complexes that orient the reacting substrate distal to the chiral ligand. Second, nucleophiles prefer to proceed through outer-sphere pathways during gold-catalyzed addition reactions to  $\pi$ -bonds. These disadvantages jeopardize the enantioselectivity of the operation. Fortunately, these challenges have been circumvented by the utilization of chiral counterions with or without a combination of chiral ligands. This section focuses on the detailed description of the seminal work of the Toste group and all other reports, which were published after the second half of 2014. For reports before 2014, please see recent reviews by the Bandini group and the Patil group. 111

Research on the use of chiral counterions in asymmetric Au(I) catalyzed reactions was spurred by the innovative work of the Toste group in 2007, which included Au(I) catalyzed intramolecular hydroalkoxylation, hydroamination, and hydrocarboxylation of allene derivatives. The arepresentative example of the intramolecular hydroalkoxylation of allenol 81 is shown in Scheme 17a. The success of this reaction hinged on the presence of dinuclear achiral [dppm(AuCl)<sub>2</sub>] complex and a silver salt of

Scheme 16. Reaction Mechanism of Au(I)-Catalyzed Cyclization Reaction of Indole-Allenoate to Form Dihydrocyclopenta Indole Derivative

the enantiomerically pure binol-based phosphate anion TRIP, Ag-(83). The corresponding 5-membered heterocyclic compound 82 was obtained in 79% yield with an excellent enantiopurity (99% enantiomeric excess (ee)). Even if it is to be determined entirely if aurophilic contacts between the individual gold centers of dinuclear gold complexes facilitate the asymmetric induction, it is highly probable that a second gold(I) center of the dinuclear gold complex could offer an additional point of interaction with the reactive site, enhancing the enantioinduction. 113 Although a detailed enantio-induction mechanism is still not clear, the formation of an intimate ion pair between the chiral counterion (chiral phosphate in most cases) and the cationic gold complex has been proposed in most other cases. Phosphate has a high pK<sub>BHX</sub> (almost the same as AcO<sup>-</sup>). 114 It is reasonable that chiral phosphate could engage in H-bonding with the incoming nucleophile OH group and hold the nucleophile in the right position for the nucleophilic attack. This interaction could generate the enantioselectivity. This strategy was further showcased in the intramolecular hydroamination of allenes that produced the required pyrrolidine derivative, in excellent yield and enantioselectivity, as shown in Scheme 17b.

The applicability of this strategy was examined further for the enantioselective intramolecular hydrocarboxylation of allenes. As shown in Scheme 17c, reactions that incorporated gold catalyst with a single chiral component (chiral gold complex or chiral counterion) resulted in poor enantioselectivity. At the same time, a gold catalyst consisting of both chiral components (chiral gold complex as well as chiral counterion) revealed the matched and mismatched pairing effect of the ligand and counterion. Despite the gold catalyst system with chiral ligand (R)-BINAP in combination with the chiral counterion (R)-83

### Scheme 17. Chiral Counterion Strategy for Enantioselective **Functionalization of Allenes**

produced chiral lactone 87 with merely 3% ee, the gold catalyst system composed of chiral ligand (S)-BINAP, which is an enantiomer with an exactly opposite stereochemistry as in the last case, and same chiral counterion (R)-83, delivered 87 in 82% ee. This result demonstrated the additive effect of chiral ligands and chiral counterions during such transformations. All the above cases showed excellent enantioselectivity and yield in the presence of very nonpolar solvents like benzene. These results clearly confirmed that the ion-pair is in operation, and enantioselectivity relies upon the proximity between the active gold(I) metal center and the chiral anion. Later, in 2010, the same group applied a chiral counterion-based catalysis strategy for the construction of a wide range of vinyl isoxazolidines 89 in high yields and excellent enantioselectivity via the intramolecular reaction between hydroxylamines and allenes. 115 A representative example is shown in Scheme 17d.

In 2015, the Toste group reported the first gold(I)-catalyzed enantioselective desymmetrization of 1,3-diols by intramolecular hydroalkoxylation of allenes, 116 a conceptually similar approach to their influential work on chiral counteranion strategy (Scheme 18). 112 Control experiments were performed on diol 91 to elucidate the mechanistic details. When chiral anion 94 was not utilized, the reaction did not proceed, confirming that the chiral silver alone cannot catalyze the hydroalkoxylation (Scheme 19a). Another set of experiments

Scheme 18. Desymmetrization of Allenyl 1,3-Diols

Scheme 19. Control Experiments to Confirm the Role of Chiral Counterion

was performed by changing the ratios of the Au/Ag (Scheme 19b). A thorough analysis of this experiment showed that dual chiral induction was not operative in the reaction due to the lesser reactivity of the gem-diaurated intermediate toward protodeauration; 43,117,118 instead, a second gold phosphate center in the dinuclear catalyst was showed a steric bias. 119 The combined results confirm the primary role of chiral counterion 94 in conferring the enantioinduction necessary for this transformation.

The power of the chiral counterion strategy in the total synthesis of natural products was recently demonstrated by Czekelius through their work on the total synthesis of enantiopure (+)-mesembrine. Their strategy was based on their previous work of desymmetrization of 1,4-diynamides. 12 When substrate 97 was treated with 99 under standardized conditions, chiral methylene pyrrolidine 98 was produced in

good yield and moderate enantiopurity. **98** was further subjected to several transformations to finally produced enantiopure (+)-mesembrine (Scheme 20). The increase in enantioselectiv-

# Scheme 20. Application of Chiral Counterion Strategy Used in Total Synthesis of (+)-Mesembrine

ity observed at lower temperatures and in nonpolar solvents suggests a possible ion-pair between the anionic chiral phosphate and cationic gold—alkyne complex. 124,125

Au(I)/chiral Brønsted acid-catalyzed enantioselective hydroamination—hydroarylation of alkynes to synthesize chiral pyrrole containing heterocyclic compounds was reported by the Patil group in 2015 (Scheme 21). <sup>126</sup> Their work postulated

Scheme 21.  $\operatorname{Au}(I)/\operatorname{Chiral}$  Brønsted Acid-Catalyzed Synthesis of 102

the necessity of tethering a hydroxyl group to the alkyne to deliver the product in high enantioselectivities. Under the optimized reaction conditions, treatment of the alcohol protected alkyne 104 with compound 100, delivered product 105 in merely 25% ee (Scheme 22a). On the other hand, when compound 106 was treated with 100 under conditions X and Y, compound 102 was obtained in almost identical yield and enantiopurity, whereas the reaction using preformed gold phosphate, generated *in situ* from JohnPhosAuMe and 103, afforded compound 102 in 95% ee (Scheme 22b). Additionally, DFT calculations were performed to determine the role of the tethered OH group and chiral phosphoric acid on the mode of

Scheme 22. Control Experiments to Determine the Role of Hydroxyl Group and Chiral Phosphoric Acid in Enantioinduction

enantioinduction. In these studies, it was observed that the maximum amount of enantioinduction could be achieved through the transition state involving the H-bonding interaction between the transient imino alcohol and chiral Brønsted acid. The bifunctional nature of the chiral phosphoric acid <sup>127,128</sup> contributed to the simultaneous activation of both the tethered hydroxyl group and the imine nitrogen atom via their hydrogenbonding interactions, producing a chiral environment and delivering products with excellent enantiopurities.

Very recently, the new approach of tethered counterion-directed catalysis (TCDC) in gold(I) catalysis was described by Marinetti and Guinchard. Contrary to the existing chiral counterion approach, this approach involves covalent tethering of the phosphate counterion to the cationic Au complex. Gold catalysis in the preceding chiral counterion strategies is mostly limited to intramolecular processes, whereas the TCDC approach can be extended to intermolecular reactions as well. A typical example of this strategy is shown in Scheme 23a. When

Scheme 23. Tandem Cycloisomerization/Nucleophilic Additions by TCDC Approach

enones 107 were treated with indole compounds 108 in the presence of 0.2 mol % of pregold catalyst 110 and 0.1 mol % of silver carbonate, products 109 were obtained in high yield and excellent enantiopurity. Even without the inclusion of the silver salt, the reaction performed well, giving enantioselectivities of up to 95% ee (Scheme 23). This shows that 110 could be considered as a source of stable Au(I) complex that can deliver the active catalyst slowly upon its interaction with nucleophiles. A plausible mechanism postulates that the Au(I) activation of the alkyne unit of 107 generates an intermediate (112), which leads to the cycloisomerization of enone, resulting in cationic intermediate 113. Intermediate 113 could exist in equilibrium with 114. The next possible event entails the nucleophilic attack of indole 108 to intermediate 113, which subsequently leads to the formation of intermediate 115. Lastly, intermediate 115 undergoes the protodeauration step to give the desired product 109. The authors hypothesized that the tight ion-pairing present in intermediate 113 is the driving force for the high enantioselectivity, as this structure represents proximity between the chiral phosphate ion and the prochiral carbon unit, which is responsible for enantio-discrimination step (Scheme 24).

# Scheme 24. Mechanistic Pathway Involved in Synthesis of 109 By TCDC Approach

### 3. ADDITIVE EFFECTS

### 3.1. Classification of Additives

Additives have been widely used in organo-transition metal catalysis with the purpose of boosting reactivity or selectivity. <sup>130,131</sup> However, to the best of our knowledge, there has been no systematic review summarizing the additive effect in gold catalysis. We believe that it is necessary to have such a review to help gold practitioners to understand the role of additives from a mechanistic perspective and thus guide them to improve the efficiency of their gold-catalyzed reactions. Truth be told, addressing the mechanistic role of an additive is complicated. In this review, we will try to offer a mechanistic perspective on the influence of an additive in a reaction whenever a mechanistic role of an additive has been invoked in the original paper(s). It is well-known that additives can take on different roles in gold

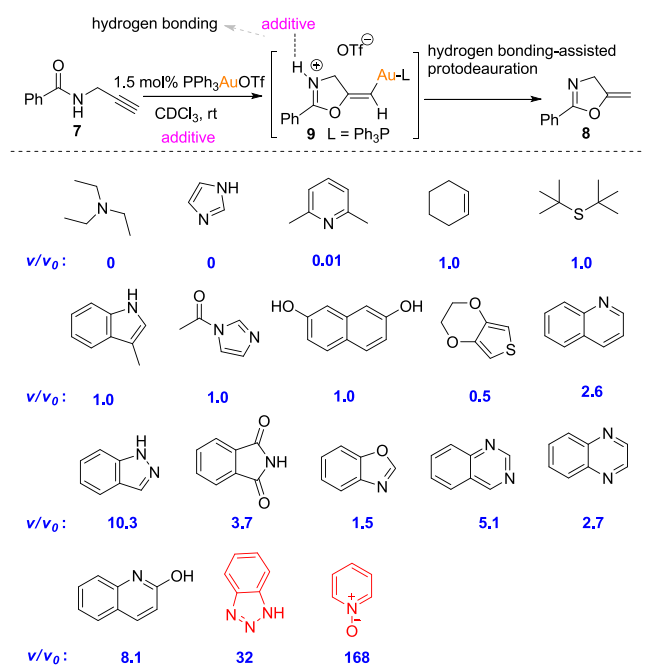
catalysis. We will confine the definition of the additive by its functional role in the catalytic process, that is, when it is added with the purpose of increasing the efficiency or the selectivity of a gold-catalyzed reaction. In our planned scenario, we will group additives into four categories: an additive that can serve as a hydrogen bonding acceptor, a gold catalyst activator, an acidic cocatalyst, or a reaction promoter. It should be noted that the additive may have multiple roles and may have a role that we do not understand yet.

### 3.2. Additives as Hydrogen Bonding Acceptors

Similar to the case of counterions, a hydrogen bond acceptor additive will facilitate the proton transfer steps in the gold catalytic cycle (Scheme 2), but a hydrogen bond acceptor additive may also act as a reversible inhibitor that could slow down stage 1 (Scheme 2) of the gold catalytic cycle because of its affinity toward cationic gold. Hence, the overall effectiveness of an additional hydrogen bond acceptor will depend on the balance between these two attributes.

In 2014, our group found that some hydrogen bonding acceptors displayed acceleration effects in some cationic gold-catalyzed reactions. We found that pyridine *N*-oxide was one of the best additives, as it increased the reaction rate 168-times in the gold-catalyzed cyclization of propargyl amide (Scheme 25).

Scheme 25. Hydrogen Bonding Acceptors in Gold-Catalyzed Cyclization of Propargyl Amide



v<sub>0</sub>: the initial reaction rate in the absence of an additive;v: the initial reaction rate in the presence of an additive

The additive effect could be rationalized from a mechanism perspective. As shown in stage 2 of the cationic gold catalytic cycle, it is difficult for the positively charged intermediate 9 to undergo protodeauration because of its positive charge. However, when additives with high hydrogen bonding basicity (measured by  $pK_{\rm BHX}$ ),  $^{92,132,133}$  rather than high  $pK_{\rm a}$ ,  $^{73}$  were added to the reaction system, the resulting hydrogen bond will reduce the positive charge on 9 and enhance the rate of the protodeauration.  $^{134,135}$  This concept is similar to a general base catalysis,  $^{136-139}$  where the additive performs as a general base.

Because hydrogen bonding acceptors also have a certain degree of gold affinity (i.e., aurophilic), these additives may compete with an alkyne/alkene substrate to complex with cationic gold. Therefore, additives will act as reversible inhibitors and will slow down, or even inhibit, stage 1 in Scheme 2. If the additive's acceleration influence outweighs its inhibitory influence, the overall effect will be positive.

Some hydrogen-bonding acceptors like triazole compounds ( $pK_{BHX} = 32$ , see Scheme 25) could establish dynamic coordination with the  $Ph_3PAu^+$  cation, which would allow for effective alkyne activation with well-improved cationic gold stability. A thermally stable triazole-Au complex (TA-Au) was developed by Shi and co-workers and used in challenging alkyne activation under harsh conditions. It also provides an alternative approach of tuning the gold catalyst reactivity. Instead of switching phosphorus ligands, the catalyst's reactivity could be modified using triazole compounds that control the equilibrium process. One such case is the gold-catalyzed Hashmi phenol 118 synthesis (Scheme 26). It had been found that

# Scheme 26. Triazole-Gold(I) Complex-Catalyzed Hashmi Phenol Synthesis

selectivity > 20:1

simple Au(I) catalysts are poor catalysts in this transformation due to their rapid decomposition. Therefore, in place of tuning the phosphorus ligands, an alternative approach was to use the 1,2,3-triazole as a coordination component to stabilize the catalyst. High chemoselectivity and yields were achieved. The kinetic profile revealed a significant reaction rate decline with an increase amount of triazoles. NMR studies offered solid evidence that the actual gold catalyst was the  $Ph_3PAu^+$ , which existed in the equilibrium with  $[Ph_3P-Au-triazole]^+$ .

The TA-Au complex was also used in propargyl ester/ether 3,3-rearrangements (Scheme 27). The isolation of the highly

# Scheme 27. Triazole-Gold(I) Complex-Catalyzed Propargyl Ester/Ether 3,3-Rearrangements

reactive allenes was failed when using ordinary cationic gold catalysts, but they can be prepared in high yields (1% catalyst loading, > 90% yields) using a triazole-gold complex. The TA-Au complex 117 also delivered effective chirality transfer without racemization over a prolonged time, providing enantioenriched allenes with high stereoselectivity (up to 99% ee with 1% gold catalyst loading).

With a triazole-gold (TA-Au) complex, the Shi group achieved several other useful synthetic transformations. Examples like the Schmittel cyclization through propargyl

vinyl ether rearrangement at room temperature (up to 77% yields, 3% catalyst loading, Scheme 28A), 143 or propargylic ester

# Scheme 28. Other Synthetic Transformation Achieved with Triazole-Gold(I) Complex

rearrangement and sequential allene hydration, giving the enones **126** with excellent yields (up to 97% yields, 0.2% catalyst loading, Scheme 28B). <sup>144</sup> Another example is the synthesis of E- $\alpha$ -haloenones **128** through propargyl acetate rearrangement and sequential allene halogenation (up to 98% yields, 1% catalyst loading, E:Z ratio >20:1 Scheme 28C). <sup>145</sup>

### 3.3. Acidic Additives for Cationic Gold Catalyst Generation

In most cases, a cationic gold catalyst containing a suitable counterion is generated *in situ* (see catalyst generation stage in Scheme 1). In the catalyst generation stage, a cationic gold catalyst LAuX (A) was created from the precatalyst LAuY through a metathesis reaction between gold halide precursors (commonly gold chloride species) and halide scavengers (commonly silver salts and others <sup>104,146</sup>). An alternative method developed by Nolan and co-workers hinges on the protonolysis of alkyl gold <sup>147</sup> or gold hydroxide <sup>55,56</sup> with various Brønsted acids. Studies have shown that excess insoluble silver salt in the reaction affects the efficiency of gold catalysis.

Our group has also developed a protocol involving Lewis acidor Brønsted acid-activation of an imido gold precatalyst (L-Au-Pht). The precatalyst (L-Au-Pht) itself is not an active gold catalyst because of its strong Au—N bond, but due to the affinity of Pht toward a Brønsted acid or Lewis acid, we were able to generate cationic gold using L—Au—Pht/acid combination. The reactivity of the L-Au-Pht/acid system could be fine-tuned with various Brønsted acids/Lewis acids. This strategy was tested in various typical Au (I) catalyzed reactions. This protocol showed superior efficiency compared with the traditional silver abstraction method in X-H (X = O, N, C) addition to C—C unsaturated compounds (Scheme 29).

As discussed above, Lewis acids can also serve as halide abstractors and thus activate gold precatalysts. Shi and coworkers reported that metal triflate Lewis acids served as a catalyst activator in gold-catalyzed reactions, in which (PMe<sub>3</sub>)-AuCl and Yb(OTf)<sub>3</sub> catalyzed the epoxy alkynes rearrangement to novel indene derivatives 138 (Scheme 30). Yb(OTf)<sub>3</sub> not only independently catalyzed the first step of the reaction involving the ring-opening of epoxy alkyne 137 to the enol alkyne 139 but also served as a *de facto* halide abstractor for the

(c)

0% (no reaction)

136

# Scheme 29. Acid Activation of Imido Gold Precatalyst Catalytic System in Typical Au(I)-Catalyzed Transformations

Scheme 30. Yb(III) Activation of Imido Gold Precatalyst Catalytic System in the Rearrangements of Epoxy Alkynes

Ph<sub>3</sub>P-Au-Pht (0.02 mol %)/ HCTf<sub>3</sub> (0.04 mol %) / 1.5 h 71% (5.6:1)

Ph<sub>3</sub>PAuCI (0.2 mol %) / AgOTf (0.4 mol %) / 1.5 h

135

second step. Control experiments showed that the  $(PMe_3)AuCl$  and  $Yb(OTf)_3$  combination probably generated  $(PMe_3)Au-(OTf)$  in situ and could have played a comparable role as that of  $[Au(PMe_3)]OTf$ . However, the combination was more effective than  $[Au(PMe_3)]OTf$  alone under the standard reaction conditions.

This approach has been exploited by Demir and co-workers in the Zn(II)/Au(I) catalyzed tandem hydroamination/annulation of 4-yne-nitriles 142 (Scheme 31).  $^{150}$   $Zn(ClO_4)_2$  was regarded as a Lewis acid that displayed the dual function of nitrile-activation and chloride ligand abstraction from  $Ph_3PAuCl$ .  $Zn(ClO_4)_2$  initiated the hydroamination step to give the intermediate 144. The subsequent nucleophilic attack of nitrogen pronucleophiles to the Au(I) activated alkyne in the intermediate 144 afforded the intermediates 145 and 146. The additional arrangement delivered 2-aminopyrroles 147 and 148.

Gandon and co-workers found that the combination of  $Cu(OTf)_2$  and  $Ph_3PAuCl$  could generate and prevent the rapid decomposition of the active cationic gold species. <sup>151,152</sup> As shown in Scheme 32, for the cyclization of the ene- $\beta$ -ketoamide 149, a reservoir for gradual (possibly reversible) delivery of

# Scheme 31. Au(I)/Zn(II) Catalyzed Tandem Hydroamination/Annulation of 4-Yne-nitriles

Scheme 32. Au(I)/Cu(II) Catalytic System in Intramolecular Hydroalkylation of Ene- $\beta$ -ketoamide

 $Ph_3PAuOTf$  could be established by the anion metathesis between  $Cu(OTf)_2$  and  $PPh_3AuCl.$  During catalysis,  $Cu(OTf)_2$  reversibly and slowly abstracts the chloride anion from the  $PPh_3AuCl$ , diminishing catalyst decomposition by maintaining a low concentration of  $Ph_3PAuOTf$ , thus allowing large-scale reactions, even at high temperatures, with low gold catalyst loading. They found that other Lewis acids like Zn(II), In(III), Bi(III) could also be good substituents.  $^{153}$ 

To investigate the generality of this strategy, the same research group also tested their approach in a variety of typical Au<sup>I</sup>-catalyzed transformations (Scheme 33).<sup>153</sup>

## 3.4. Acidic Additives for Cationic Gold Catalyst Reactivations

It has been broadly observed that most gold-catalyzed reactions have a threshold catalyst loading. This means that the reaction will not start when the catalyst loading is below a threshold amount. A possible explanation for this phenomenon is that some impurities in the reaction system, alkali or halides ingredients, for instance, deactivate the active catalyst species. <sup>154–156</sup> This explanation was confirmed when Maier pointed out that the gold affinity of OH<sup>-</sup> or Cl<sup>-</sup> is 10<sup>6</sup>-times higher than an alkyne substrate. Our group has proposed a simple method to overcome catalyst deactivation with an appropriate acid activator addition to the reaction (A in Scheme 34). <sup>157</sup> Acid activators with a high affinity toward P (impurities) may reactivate the cationic gold catalyst. In other words, an acid

# Scheme 33. Au(I)/Cu(II) Catalytic System in Other Typical Au(I)-Catalyzed Transformations

Scheme 34. Acid Additives to Reactivate the Gold Catalyst

activator (A) serves as a sacrificial reagent and interacts with possible catalyst poisons (base, halides, etc.); thus, the cationic gold can be released for catalysis (Scheme 34).

The alkenylation of arene is a representative case <sup>158</sup> (Figure 8). We found that this reaction proceeded smoothly with a high gold catalyst loading (2% vs starting material), whereas it did not proceed at all with the catalyst loading was lowered to 0.2%, in CDCl<sub>3</sub> (commercial source CDCl<sub>3</sub> used without further purification). Nevertheless, with freshly distilled CDCl<sub>3</sub>( $K_2CO_3$ -treated) as the solvent, the reaction performed well with 0.2% catalyst. <sup>157</sup> This outcome indicates that some impurities, such as chlorides, in the nondistilled CDCl<sub>3</sub> restrain the gold catalyst activity.

To better prove the influence of impurity in solvents, the same reaction was conducted with a more diluted condition ([164] concentration from 0.1 to 0.02 M but maintained 0.2% gold catalyst loading). The reaction did not proceed, even in freshly distilled CDCl<sub>3</sub>. When CD<sub>2</sub>Cl<sub>2</sub> was applied instead of CDCl<sub>3</sub> as solvent at 0.1 M, the reaction performed better (probably fewer halide impurities in the commercial CD<sub>2</sub>Cl<sub>2</sub>). Moreover, the reaction became slow if the concentration was lowered to 0.02 M. These experiments indicated that simple distillation could not remove all the impurities or the starting material 164 contains some impurities, which may poison the gold catalyst. However, common Brønsted acid, such as TfOH, can reactivate the gold catalyst (Figure 8). Lewis acids as  $In(OTf)_3$ ,  $Ag(OTf)_3$  could also reactivate the reaction, whereas others like  $Y(OTf)_3$ ,

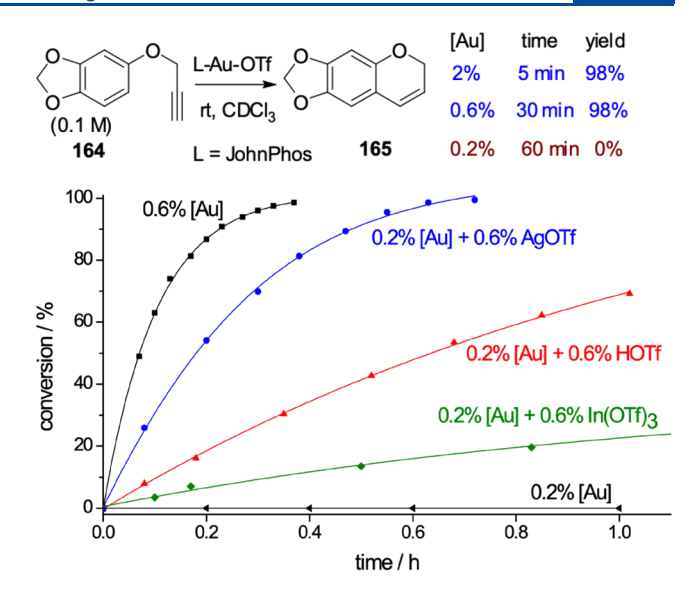


**Figure 8.** Effect of acid activators in alkenylation of arene reaction. Reproduced with permission from ref 157. Copyright 2014 American Chemical Society.

Sn(OTf)<sub>2</sub>, Zn(OTf)<sub>2</sub>, (CuOTf)<sub>2</sub>·C<sub>6</sub>H<sub>6</sub> were ineffective. Control experiments showed that a Brønsted acid or Lewis acid alone could not initiate the catalysis.

### 3.5. Acidic Additives as Co-catalysts

Some acids can also act as cocatalysts in gold-catalyzed reactions. It does not work efficiently by itself but can play a synergistic effect together with a gold catalyst in some gold-catalyzed reactions. However, Brønsted or Lewis acidic cocatalysts are not constantly effective in gold catalysis. A detailed mechanism on how acidic cocatalysts work in gold catalysis is still not clear. The possible roles of the acid cocatalyst are (a) increasing the cationic gold acidity via Lewis acid-assisted Lewis acid catalysis or Brønsted acid-assisted Lewis acid catalysis (Scheme 35a). The enhanced gold Lewis acidity

# Scheme 35. Combined Acid Catalysis in a Typical Gold Catalytic Cycle

facilitates the coordination of the cationic gold with unsaturated C–C bonds and the subsequent nucleophilic attack process (Stage 1). Besides, it could also benefit the protodeauration process (Stage 2). (b) If an acetylide-gold complex was formed, an acidic cocatalyst could convert the inert complex into the active  $\pi$ -gold-alkyne complex (Scheme 35b). (c) decreasing the active gold catalyst decay (Scheme 35c).

The effect of acids on protodeauration has been validated by the isolation and protonation of the vinylgold intermediate. We reported that vinylgold complex **166** could be readily prepared in the gold-catalyzed allenoates cyclization. <sup>161</sup> Treatment of **166** with acids of various  $pK_a$  showed that a stronger Brønsted acid led to a faster protodeauration (Scheme 36).

Scheme 36. Study of Protodeauration Using Acids of Different Strengths

In 2008, Yu established a novel glycosylation protocol using glycosyl *ortho*-alkynylbenzoates as donors, which could be activated by cationic gold catalysis.  $^{162,163}$  As illustrated in Scheme 37, activation of the alkyne in donor 168 with a gold(I)

Scheme 37. Proposed Mechanism for Gold(I)-Catalyzed Glycosidation of Glycosylo-alkynylbenzoates

Without TfOH, 10 mol % Ph<sub>3</sub>PAuOTf, 171 (yield:95%)

complex (e.g., [Ph<sub>3</sub>PAuOTf]) led to a sugar oxocarbenium ion 169 and vinylgold(I) complex 170. A nucleophilic glycosyl acceptor NuH attacks the sugar oxocarbenium species 169 and provides the target glycoside 171. The H<sup>+</sup> released from NuH then protodeaurated the vinyl gold(I) complex 170 to produce isocoumarin 172 with the regeneration of the active Au<sup>I</sup> species to complete the catalytic cycle. Yu found that a strong acid was critical for the protodeauration of this vinyl gold(I) complex 170, which regenerated the active cationic gold(I) species in the catalytic cycle. This finding has enabled the significant reduction of the loading of the gold(I) catalyst in this type of glycosylation (from the previous ca. 10 mol % to the present ca. 0.5 mol %). <sup>164</sup> The same group recently exploited this acid-assisted gold(I)-

catalyzed glycosylation approach in the synthesis of a series of natural spirostanol saponins.<sup>165</sup>

Shi and co-workers reported the first gold-catalyzed Nakamura reaction by synergistic Au(I)/Ga(III) catalysis (Scheme 38). This catalytic system is very efficient, boosting

Scheme 38. Au(I)/Ga(III) Catalytic System in Ambient Nakamura Reaction

the reaction at room temperature with the gold catalyst loading as low as 0.05% as well as up to 93% yield. The proposed mechanism stipulates that Ga(III) activates and improves the diketone nucleophilicity via Ga(III) chelation (gallium enolate formed). Experimental data showed that Ga(III) also interacted with the triazole-gold and aided to engender catalytically active species. This action might offer the reactivity to stimulate the challenging intermolecular carbon nucleophilic addition, which could not be accomplished with simple gold systems.

Guinchard and co-workers reported a regioselective synthesis of spiroindolenines (Scheme 39). They found that the addition of acetic acid as an additive to the reaction increased both the regioselectivity (179/181) and the yield of 179. The reaction was proposed to go through three pathways: coordination of the gold catalyst to the propargyl group followed by the nucleophilic attack of indole produced intermediate 178. Direct protodeauration would lead to complex 179 (pathway I:  $177 \rightarrow 178 \rightarrow 179$ ); alternatively, a 1,2-rearrangement could generate the 7-membered ring 180, and it would deliver the complex 181 after protodeauration and aromatization (pathway II:  $177 \rightarrow 178 \rightarrow 180 \rightarrow 181$ ). The intermediate 180 could also be generated from 177 directly, which delineates the possible pathway III (177  $\rightarrow$  180  $\rightarrow$  181). The addition of HOAc could facilitate the protodeauration of 178 to 179, thereby favoring 179 (pathway I) over 180 (pathway II). Computational studies showed that the

Scheme 39. Au(I)/Brønsted Acid Catalytic System for Synthesis of Spiroindolenines via Cyclizations of *N*-Propargyl Tryptamines

protonated species (HOAc as an additive) seem to be more favorable than the nonprotonated ones (without HOAc) for the conversion of 177 to 178. Additionally, a higher activation barrier was observed for the protonated species in the rearrangement of 178 to 180, which deters pathway II for the generation of 181.

Using the above strategy, the same group synthesized spirofused indoloquinuclidines 184 by a tandem Pictet–Spengler/Au<sup>I</sup>-catalyzed cyclization reaction (Scheme 40). 168

# Scheme 40. Au(I)/Brønsted Acid Catalytic System for Asymmetric Synthesis of Quinuclidines in One Pot

They found that it was difficult to achieve high conversion in the cyclization, which could be explained by the coordination of the Lewis basic bridged nitrogen atom with the cationic gold catalyst. The addition of acetic acid as an additive suppressed any competitive coordination and possibly facilitated the protodeauration step, and the reaction gave excellent yields but without diastereoselectivity. However, by switching HOAc to a chiral phosphoric acid, they could combine the acid-catalyzed asymmetric Pictet—Spengler reaction with the gold-catalyzed cyclization in one-pot, which delivered the target compounds with *ee* values of up to 90%.

Liu and co-workers also utilized a similar strategy for the synthesis of novel tetracyclic indoles containing a seven-membered ring. They reported an  $\operatorname{Au}(I)$ / trifluoroacetic acid (TFA) cocatalyzed regioselective one-pot, Michael addition/intramolecular cyclization cascade reaction (Scheme 41). The reaction was initiated by a TFA-catalyzed Michael

Scheme 41. Au(I)/Brønsted Acid Catalytic System for One-Pot Synthesis of Novel Tetracyclic Indoles Containing a Seven-Membered Ring

reaction in which the C3-position of the indole ring (186) was added to nitroolefin 185. The resulting 187, activated by Au(I), triggered a Friedel—Crafts-type alkylation at the C3-position of the indole ring and formed spirocyclic derivative 189. The intermediate 189 then rearranged through a 1,2-shift to form the seven-membered-ring complex 190, which underwent deprotonation and protodemetalation to deliver the target tetracyclic indole 191.

### 3.6. Additives as Promoters

As we discussed in Table 1, CTf<sub>3</sub><sup>-</sup> has a low gold affinity; a gold catalyst bearing this counterion could show higher reactivity in some gold-catalyzed reactions (see Table 3). However, the preparation of a catalyst with CTf<sub>3</sub><sup>-</sup> as a counterion is laborious and also unnecessary. Our group proposed that a comparable effect can be accomplished by just adding a commercial salt of KCTf<sub>3</sub> as an additive. The mechanism underlying this effect assumes that CTf<sub>3</sub><sup>-</sup> is a carbon-based soft anion liable to go through ion reshuffling with relatively soft metal centers in transition metal catalysts. For example, metal triflates (M<sup>+</sup>OTf<sup>-</sup>), or sometimes metal halides, are widely applied in cationic metal Lewis acid catalysis. When these reaction systems are added with KCTf<sub>3</sub>, the M<sup>+</sup> and OTf<sup>-</sup> interaction may diminish due to the affinity of OTf and the naked K<sup>+</sup>. This will force the ion reshuffling and thus generate a more reactive cationic species with CTf<sub>3</sub><sup>-</sup> as counterion in situ. KCTf<sub>3</sub> can be considered a promoter; as such, it will not intervene with acidic or basic species in the reaction system.

We compared the reactivity of LAuOTf/KCTf<sub>3</sub> versus LAuCTf<sub>3</sub> (Figure 9) in the 1,6-enyne cycloisomerization. The

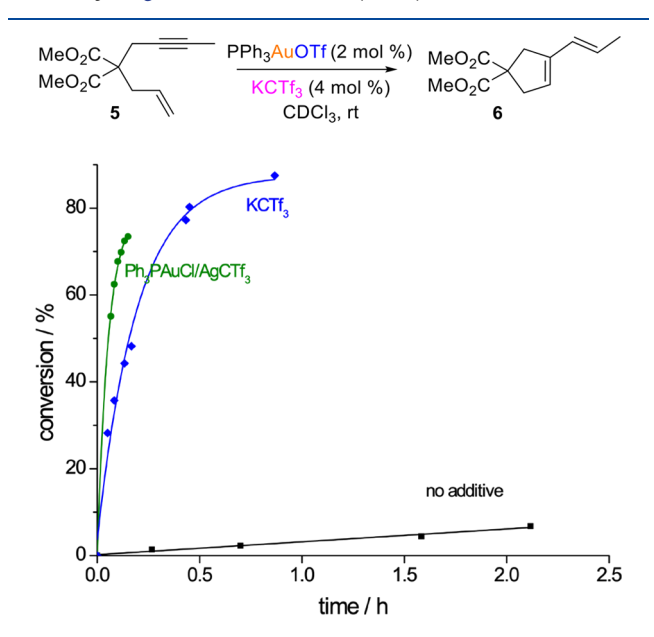


**Figure 9.** Effect of KCTf<sub>3</sub> additive in the gold-catalyzed cycloisomerization of 1,6-enyne 1. Reproduced with permission from ref 170. Copyright 2015 Royal Society of Chemistry.

reaction with KCTf $_3$  as additive was only slightly slower than the reaction of LAuCTf $_3$  prepared by treating LAuCl with AgCTf $_3$ . More importantly, this new catalytic system showed much better reactivity than the LAuOTf catalyst.

This additive effect was also applied to other gold-catalyzed reactions, in which the KCTf<sub>3</sub> promoted the reaction rate significantly (Scheme 42).

# Scheme 42. KCTf<sub>3</sub> Additive Effect in Cationic Gold-Catalyzed Reactions

# 4. SYNERGISTIC EFFECT BY LIGAND, COUNTERION, AND ADDITIVES: A CASE STUDY OF BULK AND GREEN GOLD CATALYSIS

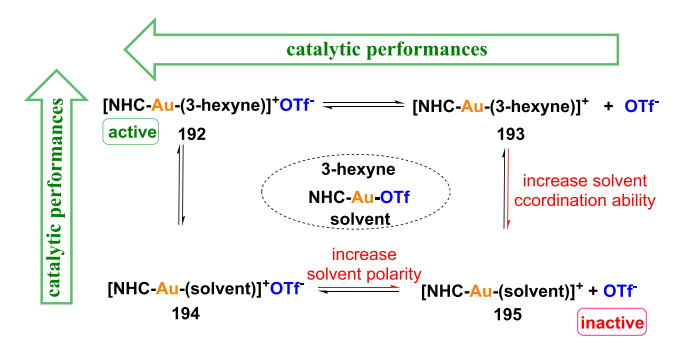
As discussed above, ligand, counterion, and additive could interplay in gold catalysis. A synergistic effect by these three factors could solve the dilemma that existed in homogeneous gold catalysis, which may direct a way to bulk and green catalysis with gold. Zuccaccia and co-workers' work has well-demonstrated this concept. They first investigated the counterion effect in all mechanistic steps of the NHC—Au—X catalyzed hydration of alkynes. The rationalization of the counterion effect enabled them to develop a highly efficient and green protocol for alkyne hydration on silver- and solvent-free conditions with suitable

ionic additives. The catalyst loading can be lowered up to 0.01 mol % relative to the substrate, which afforded high TON and TOF as well as low E-factor (Scheme 43).<sup>94</sup>

### Scheme 43. Hydration of Alkynes by Green Gold Catalysis

They then employed the optimal NHC-Au-OTf catalyst to the alkoxylation and hydration of alkynes in a group of green solvents. It was shown that TOF value decreased when the solvent polarity increased because the equilibrium was shifted toward the latter (Scheme 44); hence, the beneficial counterion

# Scheme 44. Gold Precatalyst with Alkyne and Solvent Equilibria



effect of OTf<sup>-</sup> in the nucleophilic attack (RDS) of methanol/water reduced. Alternatively, solvents containing more coordinating functional groups (such as d-limonene (C=C), propionitrile (C $\equiv$ N), and DMSO (S=O)), capable of coordination between the solvent and the metal center engendered an inactive NHC-Au (solvent) OTf species, which slowed down the reaction rate. The solvent is attacked to the solvent of the solvent

They next extended their investigation with the ligand, counterion, additive effect on the hydration of the unreactive diphenylacetylene 196 with silver-, acid-, and solvent-free conditions (Scheme 45). They observed that gold catalysts

# Scheme 45. Hydration of Diphenylacetylene by Green Gold Catalysis

with phosphine ligand showed poor activity with the catalyst deactivation occurred, while catalyst with NHC ligand gave the best performance. This was explained by the ligand stereo-electronic structure, which could regulate the acidic character of gold and thus affects the stability of the gold intermediates. Because of the lower gold affinity of OTf<sup>-</sup> to the cationic gold than OTs<sup>-</sup>, the gold catalyst with OTf<sup>-</sup> counterion performed better than the catalyst with OTs<sup>-</sup> counterion. They also found the reaction rate was improved significantly with the addition of ionic additive *n*-Bu<sub>4</sub>NOTf. The additive may function as a phase transfer catalyst transferring water to the organic phase and thus

facilitate the reaction. With the optimal condition, the catalyst loading can be lowered to 0.01 mol %, which affords hitherto the lowest E-factor (0.03) value, the highest TON (3400), and TOF  $(435 \ h^{-1})$ . These results are remarkable as they suggest that sustainable and bulk alkyne hydration reactions can be achieved with homogeneous gold catalysis.

### 5. CONCLUSION AND OUTLOOK

Counterion and additive effects in cationic gold catalysis have been widely employed in chemical syntheses. The physical properties of counterions/additives, such as their gold affinity and hydrogen bond basicity, have been invoked to rationalize reaction outcomes such as kinetics and regioselectivity. However, the exact mechanism as to which factors dictate the type or stage of a reaction, and if they pertain to the counterion or additive, remains somewhat obscure. Brønsted or Lewis acidic cocatalysts are not invariably beneficial in gold-catalyzed reactions as distinct effects are often observed with different cocatalysts. The absence of a comprehensive mechanistic understanding has hindered the rational selection of counterions and additives in gold-catalyzed reactions. The selection of a counterion for a given gold catalyst in a specific gold-catalyzed reaction is still empirical. In some cases, spectroscopic studies such as NMR, MS, and XPS have enabled insights into the behavior of additive species. Further mechanistic studies and novel control experiments are needed for a deeper understanding of the additives' role in gold catalysis.

Many gold-catalyzed reactions still suffer from low turnover numbers (TON) due to the deactivation of gold-catalysts. Counterions and additives have a significant effect on the deactivation process. However, the detailed mechanism of the deactivation process is still elusive. In some gold-catalyzed reactions such as alkyne hydration and alkyne aminations, high TON or low gold loading (at ppm level) could be easily achieved. On the other hand, the TON of some other reactions is always low. If a detailed catalyst deactivation pathway could be revealed, we might be able to design catalysts and choose reactions in a rational manner to achieve high TON.

### **AUTHOR INFORMATION**

### **Corresponding Authors**

Gerald B. Hammond — Department of Chemistry, University of Louisville, Louisville, Kentucky 40292, United States; orcid.org/0000-0002-9814-5536; Email: gb.hammond@louisville.edu

Bo Xu — College of Chemistry, Chemical Engineering and Biotechnology, Donghua University, Shanghai 201620, China; orcid.org/0000-0001-8702-1872; Email: bo.xu@dhu.edu.cn

### **Authors**

**Zhichao Lu** – Department of Chemistry, University of Louisville, Louisville, Kentucky 40292, United States; ocid.org/ 0000-0002-4746-7543

Tingting Li — College of Chemistry, Chemical Engineering and Biotechnology, Donghua University, Shanghai 201620, China Sagar R. Mudshinge — Department of Chemistry, University of Louisville, Louisville, Kentucky 40292, United States

Complete contact information is available at: https://pubs.acs.org/10.1021/acs.chemrev.0c00713

#### **Notes**

The authors declare no competing financial interest.

### **Biographies**

Zhichao Lu was born in Hubei, China, and received his B.Sc. and M.Sc. in Medicinal Chemistry from Ocean University of China. After receiving his Ph.D. degree in organic chemistry from the University of Louisville in 2018 with Professor Gerald B. Hammond and Professor Bo Xu, he started his postdoctoral research in the same research group. His current research interests involve cationic gold catalysis mechanism investigation, new fluorinating reagents, and novel fluorination methodology development.

Tingting Li was born in Jiangsu, China. She received her B.Sc. in Applied Chemistry from Yancheng Institute of Technology, China, and M.Sc. in Organic Chemistry from Donghua University, China. She is now pursuing a Ph.D. degree in Organic chemistry at Donghua University with Prof. Bo Xu. Her current research interests involve the automation of organic synthesis based on porous materials and the study of cobalt catalytic oxidation.

Sagar R. Mudshinge was born in Maharashtra, India. He received his B.Pharm. from Pune University and M.S. Pharm in Medicinal Chemistry from the National Institute of Pharmaceutical Education and Research, Mohali, India. After working for almost three years in Glenmark Pharmaceuticals, Mumbai, India, he joined the doctoral program at the University of Louisville with Professor Gerald B. Hammond. His current research interests involve the development of novel trifluoromethylation reagents and their applications.

Bo Xu was born in Hubei, China, and received his B.Sc. and M.Sc. from East China University of Science and Technology, Shanghai, China. After receiving his Ph.D. degree from the University of Louisville in 2008 (research advisor Prof. Gerald B. Hammond), he worked as a research assistant professor at the University of Louisville until 2014. He is currently a professor in the College of Chemistry, Chemical Engineering and Biotechnology, Donghua University Shanghai, China. His research interests include the development of novel and environmentally friendly synthetic methodologies, especially the synthesis of novel fluorinated building blocks for drugs and advanced materials and studies of organic reaction mechanisms.

Gerald B. Hammond was born in Lima, Perú, and received his B.Sc from the Pontifical Catholic University of Perú, his M.Sc from the University of British Columbia (Canada), and his Ph.D. from the University of Brimingham in England. Following an academic career at the University of Massachusetts Dartmouth, Professor Hammond moved to the University of Louisville in 2004, where he is currently the Endowed Chair in Organic Chemistry. His research interests include the search for new synthetic methodologies in organofluorine chemistry and other halogens, new approaches to catalysis and green chemistry, and the study of biologically active natural products from Peruvian medicinal plants.

### **ACKNOWLEDGMENTS**

We are grateful to the National Science Foundation for financial support (CHE-1855972). B.X. is grateful to the National Science Foundation of China (NSFC-21672035) for financial support. We acknowledge Luisa C. Hammond (University of Bologna, Italy) for the assistance with proofreading.

### **ABBREVIATIONS**

ACN = acetonitrile BArF = 3,5-bis(trifluoromethyl)-phenyl borate Bz = benzoate

DCE = dichloroethane

DCM = dichloromethane

dppm = bis(diphenylphosphinomethane)

ee = enantiomeric excesses

IPr = 1,3-bis(2,6-diisopropylphenyl)imidazol-2-ylidene

JohnPhos = (2-biphenyl)di-tert-butylphosphine

LA = Lewis acid

LTM = late transition metal

NHC = N-heterocyclic carbene

 $NTf_2 = bis((trifluoromethyl)sulfonyl)amide$ 

OPNB = p-nitrobenzoate

OTf = trifluoromethanesulfonate

Pht = phthalimido

RDS = rate-determining step

TA = triazole

TFA = trifluoroacetate

TOF = mol product/mol catalyst

#### REFERENCES

- (1) Bond, G. C. The Catalytic Properties of Gold. *Gold Bull.* **1972**, *5*, 11–13.
- (2) Meyer, L.-U.; de Meijere, A. Gold Catalysed Rearrangements of Strained Small Ring Hydrocarbons. *Tetrahedron Lett.* **1976**, *17*, 497–500.
- (3) Ito, Y.; Sawamura, M.; Hayashi, T. Catalytic Asymmetric Aldol Reaction: Reaction of Aldehydes with Isocyanoacetate Catalyzed by a Chiral Ferrocenylphosphine-Gold(I) Complex. *J. Am. Chem. Soc.* **1986**, 108, 6405–6406.
- (4) Fukuda, Y.; Utimoto, K. Effective Transformation of Unactivated Alkynes into Ketones or Acetals with a Gold(III) Catalyst. *J. Org. Chem.* **1991**, *56*, 3729–3731.
- (5) Teles, J. H.; Brode, S.; Chabanas, M. Cationic Gold(I) Complexes: Highly Efficient Catalysts for the Addition of Alcohols to Alkynes. *Angew. Chem., Int. Ed.* **1998**, *37*, 1415–1418.
- (6) Hashmi, A. S. K.; Frost, T. M.; Bats, J. W. Highly Selective Gold-Catalyzed Arene Synthesis. J. Am. Chem. Soc. 2000, 122, 11553–11554.
- (7) Hashmi, A. S. K.; Schwarz, L.; Choi, J.-H.; Frost, T. M. A New Gold-Catalyzed C-C Bond Formation. *Angew. Chem., Int. Ed.* **2000**, 39, 2285–2288.
- (8) Hashmi, A. S. K. Gold-Catalyzed Organic Reactions. *Chem. Rev.* 2007, 107, 3180–3211.
- (9) Arcadi, A. Alternative Synthetic Methods through New Developments in Catalysis by Gold. *Chem. Rev.* **2008**, *108*, 3266–3325.
- (10) Gorin, D. J.; Sherry, B. D.; Toste, F. D. Ligand Effects in Homogeneous Au Catalysis. *Chem. Rev.* **2008**, *108*, 3351–3378.
- (11) Li, Z.; Brouwer, C.; He, C. Gold-Catalyzed Organic Transformations. Chem. Rev. 2008, 108, 3239-3265.
- (12) Jimenez-Nunez, E.; Echavarren, A. M. Gold-Catalyzed Cycloisomerizations of Enynes: A Mechanistic Perspective. *Chem. Rev.* **2008**, *108*, 3326–3350.
- (13) Hashmi, A. S. K.; Rudolph, M. Gold Catalysis in Total Synthesis. *Chem. Soc. Rev.* **2008**, *37*, 1766–1775.
- (14) Widenhoefer, R. A. Recent Developments in Enantioselective Gold(I) Catalysis. *Chem. Eur. J.* **2008**, *14*, 5382–5391.
- (15) Garcia, P.; Malacria, M.; Aubert, C.; Gandon, V.; Fensterbank, L. Gold-Catalyzed Cross-Couplings: New Opportunities for C-C Bond Formation. *ChemCatChem* **2010**, *2*, 493–497.
- (16) Bandini, M. Gold-Catalyzed Decorations of Arenes and Heteroarenes with C-C Multiple Bonds. *Chem. Soc. Rev.* **2011**, *40*, 1358–1367.
- (17) Rudolph, M.; Hashmi, A. S. K. Gold Catalysis in Total Synthesis—an Update. *Chem. Soc. Rev.* **2012**, *41*, 2448–2462.
- (18) Brenzovich, W. E. Gold in Total Synthesis: Alkynes as Carbonyl Surrogates. *Angew. Chem., Int. Ed.* **2012**, *51*, 8933–8935.
- (19) Dorel, R.; Echavarren, A. M. Gold(I)-Catalyzed Activation of Alkynes for the Construction of Molecular Complexity. *Chem. Rev.* **2015**, *115*, 9028–9072.

- (20) Miró, J.; del Pozo, C. Fluorine and Gold: A Fruitful Partnership. Chem. Rev. 2016, 116, 11924–11966.
- (21) Zuccaccia, D.; Del Zotto, A.; Baratta, W. The Pivotal Role of the Counterion in Gold Catalyzed Hydration and Alkoxylation of Alkynes. *Coord. Chem. Rev.* **2019**, *396*, 103–116.
- (22) Lu, Z.; Hammond, G. B.; Xu, B. Improving Homogeneous Cationic Gold Catalysis through a Mechanism-Based Approach. *Acc. Chem. Res.* **2019**, 52, 1275–1288.
- (23) Gorin, D. J.; Toste, F. D. Relativistic Effects in Homogeneous Gold Catalysis. *Nature* **2007**, 446, 395–403.
- (24) Lein, M.; Rudolph, M.; Hashmi, S. K.; Schwerdtfeger, P. Homogeneous Gold Catalysis: Mechanism and Relativistic Effects of the Addition of Water to Propyne. *Organometallics* **2010**, *29*, 2206–2210.
- (25) Pernpointner, M.; Hashmi, A. S. K. Fully Relativistic, Comparative Investigation of Gold and Platinum Alkyne Complexes of Relevance for the Catalysis of Nucleophilic Additions to Alkynes. *J. Chem. Theory Comput.* **2009**, *5*, 2717–2725.
- (26) Hertwig, R. H.; Koch, W.; Schröder, D.; Schwarz, H.; Hrušák, J.; Schwerdtfeger, P. A Comparative Computational Study of Cationic Coinage Metal-Ethylene Complexes  $(C_2H_4)M^+$  (M = Cu, Ag, and Au). *J. Phys. Chem.* **1996**, *100*, 12253–12260.
- (27) Blanco Jaimes, M. C.; Böhling, C. R. N.; Serrano-Becerra, J. M.; Hashmi, A. S. K. Highly Active Mononuclear NAC-Gold(I) Catalysts. *Angew. Chem., Int. Ed.* **2013**, *52*, 7963–7966.
- (28) Veenboer, R. M. P.; Dupuy, S.; Nolan, S. P. Stereoselective Gold(I)-Catalyzed Intermolecular Hydroalkoxlation of Alkynes. *ACS Catal.* **2015**, *5*, 1330–1334.
- (29) Canseco-Gonzalez, D.; Petronilho, A.; Mueller-Bunz, H.; Ohmatsu, K.; Ooi, T.; Albrecht, M. Carbene Transfer from Triazolylidene Gold Complexes as a Potent Strategy for Inducing High Catalytic Activity. *J. Am. Chem. Soc.* **2013**, *135*, 13193–13203.
- (30) Gatto, M.; Del Zotto, A.; Segato, J.; Zuccaccia, D. Hydration of Alkynes Catalyzed by L-Au-X under Solvent- and Acid-Free Conditions: New Insights into an Efficient, General, and Green Methodology. *Organometallics* **2018**, *37*, 4685–4691.
- (31) Malhotra, D.; Mashuta, M. S.; Hammond, G. B.; Xu, B. A Highly Efficient and Broadly Applicable Cationic Gold Catalyst. *Angew. Chem., Int. Ed.* **2014**, *53*, 4456–4459.
- (32) Wang, Y.; Wang, Z.; Li, Y.; Wu, G.; Cao, Z.; Zhang, L. A General Ligand Design for Gold Catalysis Allowing Ligand-Directed Anti-Nucleophilic Attack of Alkynes. *Nat. Commun.* **2014**, *5*, 3470.
- (33) Marion, N.; Ramón, R. S.; Nolan, S. P. [(NHC)AuI]-Catalyzed Acid-Free Alkyne Hydration at Part-per-Million Catalyst Loadings. *J. Am. Chem. Soc.* **2009**, *131*, 448–449.
- (34) Hashmi, A. S. K. Homogeneous Gold Catalysis Beyond Assumptions and Proposals—Characterized Intermediates. *Angew. Chem., Int. Ed.* **2010**, *49*, 5232–5241.
- (35) Schmidbaur, H.; Schier, A. Gold  $\eta^2$ -Coordination to Unsaturated and Aromatic Hydrocarbons: The Key Step in Gold-Catalyzed Organic Transformations. *Organometallics* **2010**, 29, 2–23.
- (36) Akana, J. A.; Bhattacharyya, K. X.; Müller, P.; Sadighi, J. P. Reversible C-F Bond Formation and the Au-catalyzed Hydrofluorination of Alkynes. *J. Am. Chem. Soc.* **2007**, *129*, 7736–7737.
- (37) Flügge, S.; Anoop, A.; Goddard, R.; Thiel, W.; Fürstner, A. Structure and Bonding in Neutral and Cationic 14-Electron Gold Alkyne  $\pi$  Complexes. *Chem. Eur. J.* **2009**, *15*, 8558–8565.
- (38) Brown, T. J.; Widenhoefer, R. A. Synthesis and Equilibrium Binding Studies of Cationic, Two-Coordinate Gold(I)  $\pi$ -Alkyne Complexes. J. Organomet. Chem. **2011**, 696, 1216–1220.
- (39) Zhdanko, A.; Maier, M. E. The Mechanism of Gold(I)-Catalyzed Hydroalkoxylation of Alkynes: An Extensive Experimental Study. *Chem. Eur. J.* **2014**, *20*, 1918–1930.
- (40) Anania, M.; Jašíková, L.; Zelenka, J.; Shcherbachenko, E.; Jašík, J.; Roithová, J. Monoaurated vs. Diaurated Intermediates: Causality or Independence? *Chem. Sci.* **2020**, *11*, 980–988.
- (41) Hooper, T. N.; Green, M.; Russell, C. A. Cationic Au(I) Alkyne Complexes: Synthesis, Structure and Reactivity. *Chem. Commun.* **2010**, 46, 2313–2315.

- (42) Simonneau, A.; Jaroschik, F.; Lesage, D.; Karanik, M.; Guillot, R.; Malacria, M.; Tabet, J.-C.; Goddard, J.-P.; Fensterbank, L.; Gandon, V.; et al. Tracking Gold Acetylides in Gold(I)-catalyzed Cycloisomerization Reactions of Enynes. *Chem. Sci.* **2011**, *2*, 2417–2422.
- (43) Seidel, G.; Lehmann, C. W.; Fürstner, A. Elementary Steps in Gold Catalysis: The Significance of gem-Diauration. *Angew. Chem., Int. Ed.* **2010**, *49*, 8466–8470.
- (44) de Frémont, P.; Stevens, E. D.; Fructos, M. R.; Mar Díaz-Requejo, M.; Pérez, P. J.; Nolan, S. P. Synthesis, Isolation and Characterization of Cationic Gold(I) *N*-heterocyclic Carbene (NHC) Complexes. *Chem. Commun.* **2006**, 2045–2047.
- (45) Herrero-Gómez, E.; Nieto-Oberhuber, C.; López, S.; Benet-Buchholz, J.; Echavarren, A. M. Cationic  $\eta^1/\eta^2$ -Gold(I) Complexes of Simple Arenes. *Angew. Chem., Int. Ed.* **2006**, 45, 5455–5459.
- (46) Weber, D.; Gagné, M. R. Dinuclear Gold-Silver Resting States May Explain Silver Effects in Gold(I)-Catalysis. *Org. Lett.* **2009**, *11*, 4962–4965.
- (47) Zhu, Y.; Day, C. S.; Zhang, L.; Hauser, K. J.; Jones, A. C. A Unique Au-Ag-Au Triangular Motif in a Trimetallic Halonium Dication: Silver Incorporation in a Gold(I) Catalyst. *Chem. Eur. J.* **2013**, *19*, 12264–12271.
- (48) Wang, D.; Cai, R.; Sharma, S.; Jirak, J.; Thummanapelli, S. K.; Akhmedov, N. G.; Zhang, H.; Liu, X.; Petersen, J. L.; Shi, X. Silver Effect" in Gold(I) Catalysis: An Overlooked Important Factor. *J. Am. Chem. Soc.* **2012**, *134*, 9012–9019.
- (49) Homs, A.; Escofet, I.; Echavarren, A. M. On the Silver Effect and the Formation of Chloride-Bridged Digold Complexes. *Org. Lett.* **2013**, *15*, 5782–5785.
- (50) Tang, Y.; Yu, B. Identification of (Phosphine)gold(I) Hydrates and Their Equilibria in Wet Solutions. RSC Adv. 2012, 2, 12686–12689
- (51) Lu, Z.; Han, J.; Hammond, G. B.; Xu, B. Revisiting the Influence of Silver in Cationic Gold Catalysis: A Practical Guide. *Org. Lett.* **2015**, 17, 4534–4537.
- (52) Zhdanko, A.; Maier, M. E. Explanation of "Silver Effects" in Gold(I)-Catalyzed Hydroalkoxylation of Alkynes. *ACS Catal.* **2015**, *5*, 5994–6004.
- (53) Mizushima, E.; Hayashi, T.; Tanaka, M. Au(I)-Catalyzed Highly Efficient Intermolecular Hydroamination of Alkynes. *Org. Lett.* **2003**, *5*, 3349–3352.
- (54) Gómez-Suárez, A.; Ramón, R. S.; Slawin, A. M. Z.; Nolan, S. P. Synthetic Routes to [Au(NHC)(OH)] (NHC = *N*-heterocyclic Carbene) Complexes. *Dalton Trans.* **2012**, *41*, 5461–5463.
- (55) Gaillard, S.; Slawin, A. M. Z.; Nolan, S. P. A *N*-Heterocyclic Carbene Gold Hydroxide Complex: A Golden Synthon. *Chem. Commun.* **2010**, *46*, 2742–2744.
- (56) Gaillard, S.; Bosson, J.; Ramón, R. S.; Nun, P.; Slawin, A. M. Z.; Nolan, S. P. Development of Versatile and Silver-Free Protocols for Gold(I) Catalysis. *Chem. Eur. J.* **2010**, *16*, 13729–13740.
- (57) Tzouras, N. V.; Saab, M.; Janssens, W.; Cauwenbergh, T.; Van Hecke, K.; Nahra, F.; Nolan, S. P. Simple Synthetic Routes to N-Heterocyclic Carbene Gold(I)-Aryl Complexes: Expanded Scope and Reactivity. *Chem. Eur. J.* **2020**, 26, 5541–5551.
- (58) Gasperini, D.; Collado, A.; Goméz-Suárez, A.; Cordes, D. B.; Slawin, A. M. Z.; Nolan, S. P. Gold-Acetonyl Complexes: From Side-Products to Valuable Synthons. *Chem. Eur. J.* **2015**, *21*, 5403–5412.
- (59) Garcia, P.; Malacria, M.; Aubert, C.; Gandon, V.; Fensterbank, L. Gold-Catalyzed Cross-Couplings: New Opportunities for C-bond-C Bond Formation. *ChemCatChem* **2010**, *2*, 493–497.
- (60) Wang, W.; Hammond, G. B.; Xu, B. Ligand Effects and Ligand Design in Homogeneous Gold(I) Catalysis. *J. Am. Chem. Soc.* **2012**, 134, 5697–5705.
- (61) Benitez, D.; Tkatchouk, E.; Gonzalez, A. Z.; Goddard, W. A.; Toste, F. D. On the Impact of Steric and Electronic Properties of Ligands on Gold(I)-Catalyzed Cycloaddition Reactions. *Org. Lett.* **2009**, *11*, 4798–4801.
- (62) Jia, M.; Bandini, M. Counterion Effects in Homogeneous Gold Catalysis. *ACS Catal.* **2015**, *5*, 1638–1652.

- (63) Zeng, X.; Liu, S.; Xu, B. Stable Yet Reactive Cationic Gold Catalysts with Carbon Based Counterions. *RSC Adv.* **2016**, *6*, 77830–77833
- (64) Nieto-Oberhuber, C.; López, S.; Muñoz, M. P.; Cárdenas, D. J.; Buñuel, E.; Nevado, C.; Echavarren, A. M. Divergent Mechanisms for the Skeletal Rearrangement and [2 + 2] Cycloaddition of Enynes Catalyzed by Gold. *Angew. Chem., Int. Ed.* **2005**, *44*, 6146–6148.
- (65) Nieto-Oberhuber, C.; Muñoz, M. P.; López, S.; Jiménez-Núñez, E.; Nevado, C.; Herrero-Gómez, E.; Raducan, M.; Echavarren, A. M. Gold(I)-Catalyzed Cyclizations of 1,6-Enynes: Alkoxycyclizations and exo/endo Skeletal Rearrangements. *Chem. Eur. J.* **2006**, *12*, 1677–1693.
- (66) Mézailles, N.; Ricard, L.; Gagosz, F. Phosphine Gold(I) Bis-(trifluoromethanesulfonyl)imidate Complexes as New Highly Efficient and Air-Stable Catalysts for the Cycloisomerization of Enynes. *Org. Lett.* **2005**, *7*, 4133–4136.
- (67) Macchioni, A. Ion Pairing in Transition-Metal Organometallic Chemistry. *Chem. Rev.* **2005**, *105*, 2039–2074.
- (68) Zuccaccia, D.; Belpassi, L.; Tarantelli, F.; Macchioni, A. Ion Pairing in Cationic Olefin-Gold(I) Complexes. *J. Am. Chem. Soc.* **2009**, 131, 3170–3171.
- (69) Bucher, J.; Wurm, T.; Nalivela, K. S.; Rudolph, M.; Rominger, F.; Hashmi, A. S. K. Cyclization of Gold Acetylides: Synthesis of Vinyl Sulfonates via Gold Vinylidene Complexes. *Angew. Chem., Int. Ed.* **2014**, *53*, 3854–3858.
- (70) Nunes dos Santos Comprido, L.; Klein, J. E. M. N.; Knizia, G.; Kästner, J.; Hashmi, A. S. K. Gold(I) Vinylidene Complexes as Reactive Intermediates and Their Tendency to  $\pi$ -Backbond. *Chem. Eur. J.* **2016**, 22, 2892–2895.
- (71) Trinchillo, M.; Belanzoni, P.; Belpassi, L.; Biasiolo, L.; Busico, V.; D'Amora, A.; D'Amore, L.; Del Zotto, A.; Tarantelli, F.; Tuzi, A.; et al. Extensive Experimental and Computational Study of Counterion Effect in the Reaction Mechanism of NHC-Gold(I)-Catalyzed Alkoxylation of Alkynes. *Organometallics* **2016**, *35*, 641–654.
- (72) Marcus, Y.; Hefter, G. Ion Pairing. *Chem. Rev.* **2006**, *106*, 4585–4621.
- (73) Wang, W.; Kumar, M.; Hammond, G. B.; Xu, B. Enhanced Reactivity in Homogeneous Gold Catalysis through Hydrogen Bonding. *Org. Lett.* **2014**, *16*, 636–639.
- (74) Kumar, M.; Jasinski, J.; Hammond, G. B.; Xu, B. Alkyne/Alkene/Allene-Induced Disproportionation of Cationic Gold(I) Catalyst. *Chem. Eur. J.* **2014**, 20, 3113–3119.
- (75) Gatto, M.; Baratta, W.; Belanzoni, P.; Belpassi, L.; Del Zotto, A.; Tarantelli, F.; Zuccaccia, D. Hydration and Alkoxylation of Alkynes Catalyzed by NHC-Au-OTf. *Green Chem.* **2018**, *20*, 2125–2134.
- (76) Ciancaleoni, G.; Belpassi, L.; Zuccaccia, D.; Tarantelli, F.; Belanzoni, P. Counterion Effect in the Reaction Mechanism of NHC Gold(I)-Catalyzed Alkoxylation of Alkynes: Computational Insight into Experiment. ACS Catal. 2015, 5, 803–814.
- (77) Pihko, P. M. Hydrogen Bonding in Organic Synthesis; Wiley-VCH: Weinheim. 2009.
- (78) Yuan, B.; He, R.; Shen, W.; Li, M. Influence of Base Strength on the Proton-Transfer Reaction by Density Functional Theory. *Eur. J. Org. Chem.* **2017**, 2017, 3947–3956.
- (79) Biasiolo, L.; Ciancaleoni, G.; Belpassi, L.; Bistoni, G.; Macchioni, A.; Tarantelli, F.; Zuccaccia, D. Relationship Between the Anion/cation Relative Orientation and the Catalytic Activity of Nitrogen Acyclic Carbene-gold Catalysts. *Catal. Sci. Technol.* **2015**, *5*, 1558–1567.
- (80) Ciancaleoni, G.; Biasiolo, L.; Bistoni, G.; Macchioni, A.; Tarantelli, F.; Zuccaccia, D.; Belpassi, L. NHC-Gold-Alkyne Complexes: Influence of the Carbene Backbone on the Ion Pair Structure. *Organometallics* **2013**, 32, 4444–4447.
- (81) Zuccaccia, D.; Belpassi, L.; Macchioni, A.; Tarantelli, F. Ligand Effects on Bonding and Ion Pairing in Cationic Gold(I) Catalysts Bearing Unsaturated Hydrocarbons. *Eur. J. Inorg. Chem.* **2013**, 2013, 4121–4135.
- (82) Ciancaleoni, G.; Belpassi, L.; Tarantelli, F.; Zuccaccia, D.; Macchioni, A. A Combined NMR/DFT Study on the Ion Pair Structure

- of  $[(PR_2^1R^2)Au(\eta^2-3-hexyne)]BF_4$  Complexes. Dalton Trans. 2013, 42, 4122–4131.
- (83) Biasiolo, L.; Del Zotto, A.; Zuccaccia, D. Toward Optimizing the Performance of Homogeneous L-Au-X Catalysts through Appropriate Matching of the Ligand (L) and Counterion (X<sup>-</sup>). *Organometallics* **2015**, *34*, 1759–1765.
- (84) Schießl, J.; Schulmeister, J.; Doppiu, A.; Wörner, E.; Rudolph, M.; Karch, R.; Hashmi, A. S. K. An Industrial Perspective on Counter Anions in Gold Catalysis: Underestimated with Respect to "Ligand Effects. *Adv. Synth. Catal.* **2018**, *360*, 2493–2502.
- (85) Schießl, J.; Schulmeister, J.; Doppiu, A.; Wörner, E.; Rudolph, M.; Karch, R.; Hashmi, A. S. K. An Industrial Perspective on Counter Anions in Gold Catalysis: On Alternative Counter Anions. *Adv. Synth. Catal.* **2018**, *360*, 3949–3959.
- (86) Veenboer, R. M. P.; Collado, A.; Dupuy, S.; Lebl, T.; Falivene, L.; Cavallo, L.; Cordes, D. B.; Slawin, A. M. Z.; Cazin, C. S. J.; Nolan, S. P. Inner-Sphere versus Outer-Sphere Coordination of BF<sub>4</sub><sup>-</sup> in a NHC-Gold(I) Complex. Organometallics **2017**, *36*, 2861–2869.
- (87) Hamdoun, G.; Bour, C.; Gandon, V.; Dumez, J.-N. Empirical Estimation of the Molecular Weight of Gold Complexes in Solution by Pulsed-Field Gradient NMR. *Organometallics* **2018**, *37*, 4692–4698.
- (88) Kovács, G.; Ujaque, G.; Lledós, A. The Reaction Mechanism of the Hydroamination of Alkenes Catalyzed by Gold(I)-Phosphine: The Role of the Counterion and the N-Nucleophile Substituents in the Proton-Transfer Step. J. Am. Chem. Soc. 2008, 130, 853–864.
- (89) Zhdanko, A.; Maier, M. E. Explanation of Counterion Effects in Gold(I)-Catalyzed Hydroalkoxylation of Alkynes. *ACS Catal.* **2014**, *4*, 2770–2775.
- (90) Zhdanko, A.; Ströbele, M.; Maier, M. E. Coordination Chemistry of Gold Catalysts in Solution: A Detailed NMR Study. *Chem. Eur. J.* **2012**, *18*, 14732–14744.
- (91) Lu, Z.; Han, J.; Okoromoba, O. E.; Shimizu, N.; Amii, H.; Tormena, C. F.; Hammond, G. B.; Xu, B. Predicting Counterion Effects Using a Gold Affinity Index and a Hydrogen Bonding Basicity Index. *Org. Lett.* **2017**, *19*, 5848–5851.
- (92) Laurence, C.; Brameld, K. A.; Graton, J. r. m.; Le Questel, J.-Y.; Renault, E. The pK<sub>BHX</sub> Database: Toward a Better Understanding of Hydrogen-Bond Basicity for Medicinal Chemists. *J. Med. Chem.* **2009**, 52, 4073–4086.
- (93) An, J.; Lombardi, L.; Grilli, S.; Bandini, M. PPh<sub>3</sub>AuTFA Catalyzed in the Dearomatization of 2-Naphthols with Allenamides. *Org. Lett.* **2018**, *20*, 7380–7383.
- (94) Gatto, M.; Belanzoni, P.; Belpassi, L.; Biasiolo, L.; Del Zotto, A.; Tarantelli, F.; Zuccaccia, D. Solvent-, Silver-, and Acid-Free NHC-Au-X Catalyzed Hydration of Alkynes. The Pivotal Role of the Counterion. *ACS Catal.* **2016**, *6*, 7363–7376.
- (95) D'Amore, L.; Ciancaleoni, G.; Belpassi, L.; Tarantelli, F.; Zuccaccia, D.; Belanzoni, P. Unraveling the Anion/Ligand Interplay in the Reaction Mechanism of Gold(I)-Catalyzed Alkoxylation of Alkynes. *Organometallics* **2017**, *36*, 2364–2376.
- (96) Wu, W.-T.; Xu, R.-Q.; Zhang, L.; You, S.-L. Construction of Spirocarbocycles via Gold-Catalyzed Intramolecular Dearomatization of Naphthols. *Chem. Sci.* **2016**, *7*, 3427–3431.
- (97) Shiroodi, R. K.; Koleda, O.; Gevorgyan, V. 1,2-Boryl Migration Empowers Regiodivergent Synthesis of Borylated Furans. *J. Am. Chem. Soc.* **2014**, *136*, 13146–13149.
- (98) Yang, Y.; Li, J.; Zhu, R.; Liu, C.; Zhang, D. Theoretical Insight into Ligand- and Counterion-Controlled Regiodivergent Reactivity in Synthesis of Borylated Furans: 1,2-H vs 1,2-B Migration. *ACS Catal.* **2018**, *8*, 9252–9261.
- (99) He, Y.; Li, Z.; Tian, G.; Song, L.; Van Meervelt, L.; Van der Eycken, E. V. Gold-Catalyzed Diastereoselective Domino Dearomatization/ipso-Cyclization/aza-Michael Sequence: a Facile Access to Diverse Fused Azaspiro Tetracyclic Scaffolds. *Chem. Commun.* **2017**, *53*, 6413–6416.
- (100) Li, Y.; Zhao, X. Gold-Catalyzed Domino Cyclization Enabling Construction of Diverse Fused Azaspiro Tetracyclic Scaffolds: a Cascade Catalysis Mechanism Due to a Substrate and Counterion. *Catal. Sci. Technol.* **2020**, *10*, 2415–2426.

- (101) Brooner, R. E. M.; Brown, T. J.; Chee, M. A.; Widenhoefer, R. A. Effect of Substitution, Ring Size, and Counterion on the Intermediates Generated in the Gold-Catalyzed Intramolecular Hydroalkoxylation of Allenes. *Organometallics* **2016**, *35*, 2014–2021.
- (102) Rinaldi, A.; Petrović, M.; Magnolfi, S.; Scarpi, D.; Occhiato, E. G. Pentannulation Reaction by Tandem Gold(I)-Catalyzed Propargyl Claisen Rearrangement/Nazarov Cyclization of Enynyl Vinyl Ethers. *Org. Lett.* **2018**, *20*, 4713–4717.
- (103) Lau, V. M.; Pfalzgraff, W. C.; Markland, T. E.; Kanan, M. W. Electrostatic Control of Regioselectivity in Au(I)-Catalyzed Hydroarylation. *J. Am. Chem. Soc.* **2017**, *139*, 4035–4041.
- (104) Zhou, L.; Zhang, Y.; Fang, R.; Yang, L. Computational Exploration of Counterion Effects in Gold(I)-Catalyzed Cycloisomerization of ortho-(Alkynyl)styrenes. ACS Omega 2018, 3, 9339–9347.
- (105) Jaroschik, F.; Simonneau, A.; Lemière, G.; Cariou, K.; Agenet, N.; Amouri, H.; Aubert, C.; Goddard, J.-P.; Lesage, D.; Malacria, M.; et al. Assessing Ligand and Counterion Effects in the Noble Metal Catalyzed Cycloisomerization Reactions of 1,6-Allenynes: a Combined Experimental and Theoretical Approach. *ACS Catal.* **2016**, *6*, 5146–5160
- (106) Giacinto, P.; Cera, G.; Bottoni, A.; Bandini, M.; Miscione, G. P. DFT Mechanistic Investigation of the Gold(I)-Catalyzed Synthesis of Azepino [1,2-a] indoles. *ChemCatChem* **2015**, *7*, 2480–2484.
- (107) Yuan, B.; He, R.; Guo, X.; Shen, W.; Zhang, F.; Xu, Y.; Li, M. DFT Study on the Au(I)-Catalyzed Cyclization of Indole-Allenoate: Counterion and Solvent Effects. *New J. Chem.* **2018**, *42*, 15618–15628. (108) Carvajal, M. A.; Novoa, J. J.; Alvarez, S. Choice of Coordination Number in d<sup>10</sup> Complexes of Group 11 Metals. *J. Am. Chem. Soc.* **2004**,
- Number in d<sup>10</sup> Complexes of Group 11 Metals. J. Am. Chem. Soc. 2004, 126, 1465–1477.
- (109) Gimeno, M. C.; Laguna, A. Three- and Four-Coordinate Gold(I) Complexes. *Chem. Rev.* **1997**, *97*, 511–522.
- (110) Schwerdtfeger, P.; Hermann, H. L.; Schmidbaur, H. Stability of the Gold(I)-Phosphine Bond. A Comparison with Other Group 11 Elements. *Inorg. Chem.* **2003**, *42*, 1334–1342.
- (111) Inamdar, S. M.; Konala, A.; Patil, N. T. When Gold Meets Chiral Brønsted Acid Catalysts: Extending the Boundaries of Enantioselective Gold Catalysis. *Chem. Commun.* **2014**, *50*, 15124–15135.
- (112) Hamilton, G. L.; Kang, E. J.; Mba, M.; Toste, F. D. A Powerful Chiral Counterion Strategy for Asymmetric Transition Metal Catalysis. *Science* **2007**, 317, 496–499.
- (113) Teller, H.; Corbet, M.; Mantilli, L.; Gopakumar, G.; Goddard, R.; Thiel, W.; Fürstner, A. One-Point Binding Ligands for Asymmetric Gold Catalysis: Phosphoramidites with a TADDOL-Related but Acyclic Backbone. *J. Am. Chem. Soc.* **2012**, *134*, 15331–15342.
- (114) Pike, S. J.; Hutchinson, J. J.; Hunter, C. A. H-Bond Acceptor Parameters for Anions. J. Am. Chem. Soc. 2017, 139, 6700–6706.
- (115) LaLonde, R. L.; Wang, Z. J.; Mba, M.; Lackner, A. D.; Toste, F. D. Gold(I)-Catalyzed Enantioselective Synthesis of Pyrazolidines, Isoxazolidines, and Tetrahydrooxazines. *Angew. Chem., Int. Ed.* **2010**, 49, 598–601.
- (116) Zi, W.; Toste, F. D. Gold(I)-Catalyzed Enantioselective Desymmetrization of 1,3-Diols through Intramolecular Hydroalkoxylation of Allenes. *Angew. Chem., Int. Ed.* **2015**, *54*, 14447–14451.
- (117) Brown, T. J.; Weber, D.; Gagné, M. R.; Widenhoefer, R. A. Mechanistic Analysis of Gold(I)-Catalyzed Intramolecular Allene Hydroalkoxylation Reveals an Off-Cycle Bis(gold) Vinyl Species and Reversible C-O Bond Formation. *J. Am. Chem. Soc.* **2012**, *134*, 9134–9137.
- (118) Weber, D.; Jones, T. D.; Adduci, L. L.; Gagné, M. R. Strong Electronic and Counterion Effects on Geminal Digold Formation and Reactivity as Revealed by Gold(I)-Aryl Model Complexes. *Angew. Chem., Int. Ed.* **2012**, *51*, 2452–2456.
- (119) Bandini, M.; Bottoni, A.; Chiarucci, M.; Cera, G.; Miscione, G. P. Mechanistic Insights into Enantioselective Gold-Catalyzed Allylation of Indoles with Alcohols: The Counterion Effect. *J. Am. Chem. Soc.* **2012**, *134*, 20690–20700.

- (120) Brooner, R. E. M.; Widenhoefer, R. A. Synthesis and Structure of Dicationic, Bis(gold)  $\pi$ -Alkene Complexes Containing a 2,2′-Bis(phosphino)biphenyl Ligand. *Organometallics* **2012**, 31, 768–771.
- (121) Kim, J. H.; Park, S.-W.; Park, S. R.; Lee, S.; Kang, E. J. Counterion-Mediated Hydrogen-Bonding Effects: Mechanistic Study of Gold(I)-Catalyzed Enantioselective Hydroamination of Allenes. *Chem. Asian J.* **2011**, *6*, 1982–1986.
- (122) Spittler, M.; Lutsenko, K.; Czekelius, C. Total Synthesis of (+)-Mesembrine Applying Asymmetric Gold Catalysis. *J. Org. Chem.* **2016**, *81*, 6100–6105.
- (123) Mourad, A. K.; Leutzow, J.; Czekelius, C. Anion-Induced Enantioselective Cyclization of Diynamides to Pyrrolidines Catalyzed by Cationic Gold Complexes. *Angew. Chem., Int. Ed.* **2012**, *51*, 11149–11152
- (124) Hashmi, A. S. K. Raising the Gold Standard. *Nature* **2007**, 449, 292–293.
- (125) Salvi, N.; Belpassi, L.; Zuccaccia, D.; Tarantelli, F.; Macchioni, A. Ion Pairing in NHC Gold(I) Olefin Complexes: A Combined Experimental/Theoretical Study. *J. Organomet. Chem.* **2010**, *695*, 2679–2686.
- (126) Shinde, V. S.; Mane, M. V.; Vanka, K.; Mallick, A.; Patil, N. T. Gold(I)/Chiral Brønsted Acid Catalyzed Enantioselective Hydroamination-Hydroarylation of Alkynes: The Effect of a Remote Hydroxyl Group on the Reactivity and Enantioselectivity. *Chem. Eur. J.* **2015**, *21*, 975–979.
- (127) Mutyala, A. K.; Patil, N. T. Enantioselective Heterogeneous Brønsted Acid Catalysis. *Org. Chem. Front.* **2014**, *1*, 582–586.
- (128) Akiyama, T. Stronger Brønsted Acids. Chem. Rev. 2007, 107, 5744-5758.
- (129) Zhang, Z.; Smal, V.; Retailleau, P.; Voituriez, A.; Frison, G.; Marinetti, A.; Guinchard, X. Tethered Counterion-Directed Catalysis: Merging the Chiral Ion-Pairing and Bifunctional Ligand Strategies in Enantioselective Gold(I) Catalysis. *J. Am. Chem. Soc.* **2020**, *142*, 3797–3805.
- (130) Wang, C.; Xi, Z. Co-Operative Effect of Lewis Acids with Transition Metals for Organic Synthesis. *Chem. Soc. Rev.* **2007**, *36*, 1395–1406.
- (131) Becica, J.; Dobereiner, G. E. The Roles of Lewis Acidic Additives in Organotransition Metal Catalysis. *Org. Biomol. Chem.* **2019**, *17*, 2055–2069.
- (132) Okoromoba, O. E.; Han, J.; Hammond, G. B.; Xu, B. Designer HF-Based Fluorination Reagent: Highly Regioselective Synthesis of Fluoroalkenes and gem-Difluoromethylene Compounds from Alkynes. *J. Am. Chem. Soc.* **2014**, *136*, 14381–14384.
- (133) Han, J.; Lu, Z.; Flach, A. L.; Paton, R. S.; Hammond, G. B.; Xu, B. Role of Hydrogen-Bonding Acceptors in Organo-Enamine Catalysis. *Chem. Eur. J.* **2015**, *21*, 11687–11691.
- (134) Laurence, C.; Graton, J. r. m.; Berthelot, M.; Besseau, F. o.; Le Questel, J.-Y.; Luçon, M.; Ouvrard, C.; Planchat, A. l.; Renault, E. An Enthalpic Scale of Hydrogen-Bond Basicity. 4. Carbon  $\pi$  Bases, Oxygen Bases, and Miscellaneous Second-Row, Third-Row, and Fourth-Row Bases and a Survey of the 4-Fluorophenol Affinity Scale. *J. Org. Chem.* **2010**, 75, 4105–4123.
- (135) Reed, A. E.; Curtiss, L. A.; Weinhold, F. Intermolecular Interactions from a Natural Bond Orbital, Donor-Acceptor Viewpoint. *Chem. Rev.* **1988**, *88*, 899–926.
- (136) Ault, A. General Acid and General Base Catalysis. *J. Chem. Educ.* **2007**, *84*, 38–39.
- (137) Kwan, E. E. The Rate of Proton Transfer. J. Chem. Educ. 2007, 84, 39.
- (138) Wilson, T. J.; Li, N.-S.; Lu, J.; Frederiksen, J. K.; Piccirilli, J. A.; Lilley, D. M. J. Nucleobase-mediated General Acid-base Catalysis in the Varkud Satellite Ribozyme. *Proc. Natl. Acad. Sci. U. S. A.* **2010**, *107*, 11751–11756.
- (139) Kath-Schorr, S.; Wilson, T. J.; Li, N.-S.; Lu, J.; Piccirilli, J. A.; Lilley, D. M. J. General Acid-Base Catalysis Mediated by Nucleobases in the Hairpin Ribozyme. *J. Am. Chem. Soc.* **2012**, *134*, 16717–16724. (140) Duan, H.; Sengupta, S.; Petersen, J. L.; Akhmedov, N. G.; Shi, X. Triazole-Au(I) Complexes: A New Class of Catalysts with Improved

- Thermal Stability and Reactivity for Intermolecular Alkyne Hydro-amination. J. Am. Chem. Soc. 2009, 131, 12100–12102.
- (141) Chen, Y.; Yan, W.; Akhmedov, N. G.; Shi, X. 1,2,3-Triazole as a Special "X-Factor" in Promoting Hashmi Phenol Synthesis. *Org. Lett.* **2010**, *12*, 344–347.
- (142) Wang, D.; Gautam, L. N. S.; Bollinger, C.; Harris, A.; Li, M.; Shi, X. 1,2,3-Triazole Bound Au(I) (TA-Au) as Chemoselective Catalysts in Promoting Asymmetric Synthesis of Substituted Allenes. *Org. Lett.* **2011**, *13*, 2618–2621.
- (143) Wang, Q.; Aparaj, S.; Akhmedov, N. G.; Petersen, J. L.; Shi, X. Ambient Schmittel Cyclization Promoted by Chemoselective Triazole-Gold Catalyst. *Org. Lett.* **2012**, *14*, 1334–1337.
- (144) Wang, D.; Zhang, Y.; Harris, A.; Gautam, L. N. S.; Chen, Y.; Shi, X. Triazole-Gold-Promoted, Effective Synthesis of Enones from Propargylic Esters and Alcohols: A Catalyst Offering Chemoselectivity, Acidity and Ligand Economy. *Adv. Synth. Catal.* **2011**, 353, 2584–2588
- (145) Wang, D.; Ye, X.; Shi, X. Efficient Synthesis of E- $\alpha$ -Haloenones Through Chemoselective Alkyne Activation Over Allene with Triazole-Au Catalysts. *Org. Lett.* **2010**, *12*, 2088–2091.
- (146) Wegener, M.; Huber, F.; Bolli, C.; Jenne, C.; Kirsch, S. F. Silver-Free Activation of Ligated Gold(I) Chlorides: The Use of [Me<sub>3</sub>NB<sub>12</sub>Cl<sub>11</sub>]- as a Weakly Coordinating Anion in Homogeneous Gold Catalysis. *Chem. Eur. J.* **2015**, *21*, 1328–1336.
- (147) Nieto-Oberhuber, C.; Muñoz, M. P.; Buñuel, E.; Nevado, C.; Cárdenas, D. J.; Echavarren, A. M. Cationic Gold(I) Complexes: Highly Alkynophilic Catalysts for the exo- and endo-Cyclization of Enynes. *Angew. Chem., Int. Ed.* **2004**, *43*, 2402–2406.
- (148) Han, J.; Shimizu, N.; Lu, Z.; Amii, H.; Hammond, G. B.; Xu, B. Efficient Generation and Increased Reactivity in Cationic Gold via Brønsted Acid or Lewis Acid Assisted Activation of an Imidogold Precatalyst. *Org. Lett.* **2014**, *16*, 3500–3503.
- (149) Dai, L.-Z.; Shi, M. Gold(I)- and Yb(OTf)<sub>3</sub>-Cocatalyzed Rearrangements of Epoxy Alkynes: Transfer of a Carbonyl Group in a Five-Membered Carbocycle. *Chem. Eur. J.* **2010**, *16*, 2496–2502.
- (150) Demir, A. S.; Emrullahoglu, M.; Buran, K. Gold(I)/Zn(II) Catalyzed Tandem Hydroamination/Annulation Reaction of 4-ynenitriles. *Chem. Commun.* **2010**, *46*, 8032–8034.
- (151) Guérinot, A.; Fang, W.; Sircoglou, M.; Bour, C.; Bezzenine-Lafollée, S.; Gandon, V. Copper Salts as Additives in Gold(I)-Catalyzed Reactions. *Angew. Chem., Int. Ed.* **2013**, *52*, 5848–5852.
- (152) Bour, C.; Gandon, V. New Procedures for Catalytic Carbophilic Activation by Gold and Gallium  $\pi$ -Acids. Synlett **2015**, 26, 1427–1436.
- (153) Fang, W.; Presset, M.; Guérinot, A.; Bour, C.; Bezzenine-Lafollée, S.; Gandon, V. Silver-Free Two-Component Approach in Gold Catalysis: Activation of [LAuCl] Complexes with Derivatives of Copper, Zinc, Indium, Bismuth, and Other Lewis Acids. *Chem. Eur. J.* **2014**, *20*, 5439–5446.
- (154) Oxford, S. M.; Henao, J. D.; Yang, J. H.; Kung, M. C.; Kung, H. H. Understanding the Effect of Halide Poisoning in CO Oxidation over Au/TiO<sub>2</sub>. *Appl. Catal., A* **2008**, 339, 180–186.
- (155) Chandler, B. D.; Kendell, S.; Doan, H.; Korkosz, R.; Grabow, L. C.; Pursell, C. J. NaBr Poisoning of Au/TiO<sub>2</sub> Catalysts: Effects on Kinetics, Poisoning Mechanism, and Estimation of the Number of Catalytic Active Sites. *ACS Catal.* **2012**, *2*, 684–694.
- (156) Bartholomew, C. H. Mechanisms of Catalyst Deactivation. *Appl. Catal., A* **2001**, 212, 17–60.
- (157) Kumar, M.; Hammond, G. B.; Xu, B. Cationic Gold Catalyst Poisoning and Reactivation. *Org. Lett.* **2014**, *16*, 3452–3455.
- (158) Nevado, C.; Echavarren, A. M. Intramolecular Hydroarylation of Alkynes Catalyzed by Platinum or Gold: Mechanism and endo Selectivity. *Chem. Eur. J.* **2005**, *11*, 3155–3164.
- (159) Burfield, D. R.; Goh, E. H.; Ong, E. H.; Smithers, R. H. Storage and Decomposition of Chloroform. *Gazz. Chim. Ital.* **1983**, *113*, 841–3.
- (160) Barrio, P.; Kumar, M.; Lu, Z.; Han, J.; Xu, B.; Hammond, G. B. Acidic Co-Catalysts in Cationic Gold Catalysis. *Chem. Eur. J.* **2016**, 22, 16410–16414.

- (161) Liu, L.-P.; Xu, B.; Mashuta, M. S.; Hammond, G. B. Synthesis and Structural Characterization of Stable Organogold(I) Compounds. Evidence for the Mechanism of Gold-Catalyzed Cyclizations. *J. Am. Chem. Soc.* **2008**, *130*, 17642–17643.
- (162) Yu, B. Gold(I)-Catalyzed Glycosylation with Glycosyl o-Alkynylbenzoates as Donors. *Acc. Chem. Res.* **2018**, *51*, 507–516.
- (163) Li, Y.; Yang, Y.; Yu, B. An Efficient Glycosylation Protocol with Glycosyl Ortho-Alkynylbenzoates as Donors under the Catalysis of Ph<sub>3</sub>PAuOTf. *Tetrahedron Lett.* **2008**, *49*, 3604–3608.
- (164) Zhu, Y.; Yu, B. Characterization of the Isochromen-4-yl-gold(I) Intermediate in the Gold(I)-Catalyzed Glycosidation of Glycosyl ortho-Alkynylbenzoates and Enhancement of the Catalytic Efficiency Thereof. *Angew. Chem., Int. Ed.* **2011**, *50*, 8329–8332.
- (165) Ehianeta, T. S.; Shen, D.; Xu, P.; Yu, B. Synthesis of Spirostanol Saponins via Gold(I)-Catalyzed Glycosylation in the Presence of Ga(OTf)<sub>3</sub>, In(OTf)<sub>3</sub>, or HOTf. Chin. J. Chem. **2019**, *37*, 827–833.
- (166) Xi, Y.; Wang, D.; Ye, X.; Akhmedov, N. G.; Petersen, J. L.; Shi, X. Synergistic Au/Ga Catalysis in Ambient Nakamura Reaction. *Org. Lett.* **2014**, *16*, 306–309.
- (167) Magné, V.; Marinetti, A.; Gandon, V.; Voituriez, A.; Guinchard, X. Synthesis of Spiroindolenines via Regioselective Gold(I)-Catalyzed Cyclizations of N-Propargyl Tryptamines. *Adv. Synth. Catal.* **2017**, 359, 4036–4042.
- (168) Glinsky-Olivier, N.; Retailleau, P.; Guinchard, X. Gold-Catalyzed Synthesis of Spirofused Indoloquinuclidines. *Eur. J. Org. Chem.* **2018**, 2018, 5823–5829.
- (169) Xu, S.; Zhou, Y.; Xu, J.; Jiang, H.; Liu, H. Gold-Catalyzed Michael Addition/Intramolecular Annulation Cascade: an Effective Pathway for the Chemoselective- and Regioselective Synthesis of Tetracyclic Indole Derivatives in Water. *Green Chem.* **2013**, *15*, 718–726.
- (170) Han, J.; Lu, Z.; Wang, W.; Hammond, G. B.; Xu, B. Potassium Tris(triflyl)methide (KCTf<sub>3</sub>): a Broadly Applicable Promoter for Cationic Metal Catalysis. *Chem. Commun.* **2015**, *51*, 13740–13743.